

**A SLOPE-DEPENDENT DISJOINING PRESSURE
FOR LENNARD-JONES LIQUID FILMS**

A Thesis
Submitted to the Graduate Faculty of the
Louisiana State University and
Agricultural and Mechanical College
In partial fulfillment of the
Requirements for the degree of
Master of Science in Mechanical Engineering

in

The Department of Mechanical Engineering

by
Taeil Yi
B.S. Hanyang University, 2003
December 2005

ACKNOWLEDGMENTS

The author would like to thank his major professor, Dr. Harris Wong. Without for his continuous encouragement, insightful suggestions, devoted guidance, and constructive suggestions, the research work and preparation of this thesis could not be done progressively.

The author would also like to thank Dr. D. Moldovan and Dr. Y.A. Antipov for their inspiring suggestions, their time and effort to serve on his examination committee.

The author would also like to thank his colleagues in lab: Donghong Min, Jin Zhang, and Ping Du for their help and great time they spent together.

Finally, the author wants to specially thank his fiancée Jina Kim, for the heroic efforts, constant love, and encouragement. In addition, the author wants to express particular gratefulness to his parents Sangwoon Lee and Jungsuk Kim, his brother Kyungtae Lee, and his friends Sangsoo Lee and Daehyung Kim, for their firm and continuous love and support.

TABLE OF CONTENTS

ACKNOWLEDGMENTS.....	ii
LIST OF FIGURES.....	v
ABSTRACT.....	vi
CHAPTER 1. INTRODUCTION.....	1
CHAPTER 2. DERIVATION OF DISJOINING PRESSURE.....	5
CHAPTER 3. BOUNDARY CONDITIONS... ..	11
CHAPTER 4. AUGMENTED YOUNG-LAPLACE EQUATION.....	13
CHAPTER 5. UNIFORM FILM SOLUTIONS.....	15
CHAPTER 6. EQUILIBRIUM DROP PROFILES.....	19
CHAPTER 7. STABILITY ANALYSIS OF UNIFORM FILMS.....	25
CHAPTER 8. DISCUSSIONS AND CONCLUSIONS.....	28
REFERENCES.....	29
APPENDICES	
A. Integration of the intermolecular potential.... ..	32
B. Excess energy and interaction potential.....	38
C. Analytical solution of uniform films.....	42
D. Perturbation solutions of precursor film.....	45
E. Asymptotic solutions of precursor film thickness and C_2	48
F. Relations between two critical capillary pressures (C_1, C_2).....	49
G. Computer programs.....	51
G.1. The forth order Runge-Kutta code.....	51

G.2. Maple code for Appendix A and B.....	55
G.3. Boundary conditions at the contact point.....	63
VITA.....	66

LIST OF FIGURES

Figure 2.1 A liquid drop on a solid substrate in thermodynamic equilibrium.....	6
Figure 2.2 A wedge liquid film located near a solid substrate in the cylindrical coordinate where the wedge slope is ψ	7
Figure 5.1 Numerical solutions versus asymptotic solutions for the precursor film thickness....	17
Figure 6.1 Depending on the parameter C , the drop profile can be divided into seven groups....	19
Figure 6.2 Effect of δ on drop profiles.....	20
Figure 6.3 Pseudo partial wetting drop profiles for different ε and R	22
Figure 6.4 Film profiles for fixed $R\xi^{10} / \varepsilon$	23
Figure 6.5 Period versus C for drops connected by a thin film for fixed intermolecular potential parameters $(\varepsilon, R\xi^{10})$	24
Figure 6.6 Area per period versus C for drops connected by a thin film for fixed $(\varepsilon, R\xi^{10})$	24

ABSTRACT

A molecule in a bulk liquid is subject to intermolecular forces. A molecule in a thin liquid film may experience additional intermolecular forces, if the thin film thickness h is less than roughly 100 nm. The additional forces arise from the molecule's proximity to different materials or phases sandwiching the thin film. The effect of these intermolecular forces at the continuum level is captured by disjoining pressure Π . Since Π dominates at small film thickness, it determines the stability and wettability of thin films. To leading order, $\Pi = \Pi(h)$ because thin films are generally uniform. This form, however, can not be applied to films that end at the substrate with non-zero contact angles. Recently, a new procedure for deriving disjoining-pressure expressions has been developed (Wu and Wong 2004). In this approach, the total energy of a drop on a solid substrate is minimized. The total energy contains an interaction energy, which is found by pairwise summation of van der Waals potentials. Minimization of the total energy yields $\Pi = \Pi(h, h_x, h_{xx})$. The current work extends the summation to the Lennard-Jones potential. Disjoining pressure $\Pi = \Pi(h, h_x, h_{xx})$ is also found, but the new expression accepts a much larger class of equilibrium drop and meniscus shapes. For example, a drop can have a precursor film of a finite or infinite extent and two drops can be connected by a precursor film and the unit repeats periodically. The last section discusses the stability of uniform films and the influence of intermolecular potential parameters.

CHAPTER 1. INTRODUCTION

A macroscopic liquid film on a solid substrate can be analyzed by the macroscopic properties such as viscosity, capillarity, and gravity (Hocking 1993). However, additional forces must be considered if the range of film thickness is under 100nm. These forces come from inter-atomic activities between the liquid molecules and the solid or vapor molecules surrounding the thin-film. If the liquid-solid attraction is stronger than the corresponding liquid-liquid attraction, then the additional forces will be attractive, and vice versa. These thin-film forces affect the film shape. For example, gas bubbles in contact with each other in a surfactant-filled liquid are stable for a long time. The lamellar films separating the bubbles tend to become thinner due to the pressure difference. However, there exists a force that prevents the thickness of this film from decreasing. This repulsive force between surfaces is called disjoining pressure Π . Derjaguin and Titijevskaya (1957) found that the disjoining pressure balances the capillary pressure and is equal to the pressure differences between the normal pressure in the film and the liquid pressure. By using Derjaguin's approximation (Israelachvili 2002), the interactive force is directly calculated from the potential energy. Due to this fact, disjoining pressure is also referred to as the change of Helmholtz free energy per unit area for closed thermodynamic systems.

Many researchers (Oron et al. 1997, de Gennes et al. 2003, Davis and Troian 2003) have

studied thin films by using disjoining pressure $\Pi = A/6\pi h^3$, where A is the Hamaker constant. They have calculated models equilibrium profiles of uniform and non-uniform films and film breakage. However, this disjoining pressure is divergent if $h \rightarrow 0$ and this limitation cast doubt on its validity when a liquid film ends on a substrate. Thus, some researchers focused on the microscopic area near the end of the film on a substrate. Miller and Ruckenstein (1974) calculated contact angle dependent intermolecular interactions of a liquid wedge on a solid substrate. However, this expression is only a function of the film thickness. This disjoining pressure Π is given as $\Pi = -dP/dh$ where P is the long-range tail of the energy of a flat liquid film of thickness h . Hocking (1993) considered a disjoining pressure model that depends on including both the height and the slope of a liquid film assuming van der Waals attractive potential. However, the intermolecular potential in his model does not imply equilibrium although the potential is constant at the interface. In addition, the relation between disjoining pressure and intermolecular potential is not clear and the contact line can move without slip. Wu and Wong (2004) remedied this problem by using a rigorous derivation procedure. To demonstrate ultra thin-film phenomena, their model needs another terms in addition to the long-range attractive component. Here, by using the Lennard-Jones potential, a short-range repulsive component is added. Repulsive potentials play an important role in ultra thin-film phenomena. Verlet (1972) showed the important roles of repulsive forces in the Lennard-Jones liquid and

Weeks et al. (1971) used this assumption to find the effects of repulsive forces in constructing the equilibrium structure of liquid. The Lennard-Jones potential can be used as a model for monatomic liquids, such as He and Ar.

Brochard-Wyart et al. (1991) classified drop shapes into three categories depending on two factors: Hamaker constant (A) which describes van der Waals interactions, and the spreading coefficient (S) controlled by the short range potential. By varying these two factors (A and S), drops are divided into three different states: complete wetting, pseudo partial wetting, and partial wetting. Brochard-Wyart et al. (1991) also theoretically proved a pseudo partial wetting case by investigating the free energy of the system. Many experimental research papers have supported dewetting phenomenon by using various materials (Silberzan & Leger 1991, Moon et al. 2004, Gokhale et al. 2004). They followed the definition of pseudo partial wetting as a spreading film in equilibrium with a non-zero finite contact angle (Brochard-Wyart et al. 1991). Reiter et al. (1999) demonstrated the equilibrium state schematically by using different cases of Gibbs free energy.

This work extends the study of Wu and Wong (2004) by replacing the van der Waals potential by the Lennard-Jones potential. Both excess energy and disjoining pressure isotherms are developed by using this new model. The Lennard-Jones model is needed to form a precursor film because existence of this ultra thin-film depends on the repulsive component of the potential.

The augmented Young-Laplace equation yields various drop shapes, including that of pseudo partial wetting, by controlling the pressure difference. In addition, the stability of uniform films is analyzed.

CHAPTER 2. DERIVATION OF DISJOINING PRESSURE

Consider a mono-atomic liquid drop without charge on a smooth solid surface and in thermodynamic equilibrium with its own vapor at constant temperature, as illustrated in Fig. 2.1

The drop size is assumed small to neglect gravitational effects and the interface is located following the Gibbs model. The total energy of the system is fundamentally driven by thermodynamic equilibrium (Yeh et al. 1999). The drop is also assumed to be two dimensional and symmetry. In this system, the total energy consists of surface energies and an excess interaction potential energy E . The mass of the liquid drop and the temperature of the system are constant. After applying the symmetry condition, the energy of this system is obtained by considering half of the drop from the center of symmetry to the end of the liquid drop. In addition, the total energy of molecules is minimized when the system reaches equilibrium. To identify this minimum energy state, a variation method is used and the variation of this total energy is null (Morse and Feshback 1953, Courant and Hilbert 1953) :

$$\delta \int_0^{x_0} \left[\sigma \left(1 + h_x^2 \right)^{1/2} + \sigma_{fs} - \sigma_{sg} + E + p_c h \right] dx = 0 \quad , \quad (2.1)$$

where δ represents the variation of a functional, h is the film height, x is a horizontal coordinate starting at the center of the drop, h_x is the slope at x , and σ is the liquid-vapor interfacial surface tension. The arc length of a liquid-vapor interfacial element is $\left(1 + h_x^2 \right)^{1/2}$, the half width of

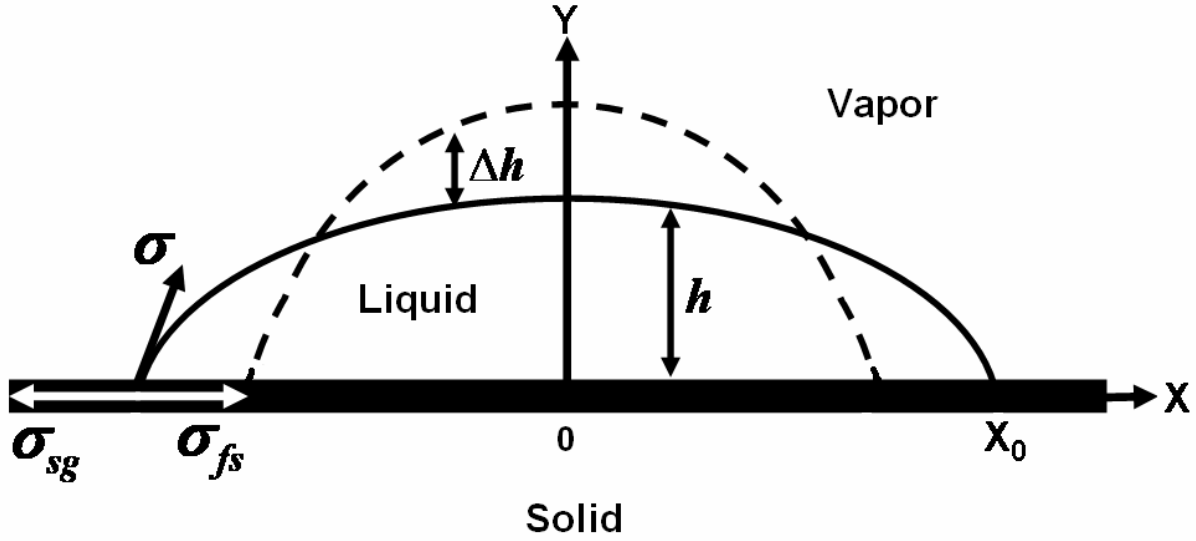


Figure 2.1 A liquid drop on a solid substrate in thermodynamic equilibrium. The drop is symmetric at constant temperature. This system is located in a closed box. The difference between the equilibrium and fluctuated shapes is denoted by Δh .

the drop is x_0 , σ_{fs} and σ_{sg} are surface energies between liquid and solid and between solid and gas, E is excess energy due to thin-film forces and depends on the film thickness and slope, and p_c is a Lagrange multiplier. The term $p_c h$ imposes mass conservation. This free energy expression has an entropy component. However, this component is canceled after substituting the energy balance into the Helmholtz free energy function (Kittel & Kroemer 1980, Ash et al. 1973, Butt et al. 2003). After applying Leibniz rule, Eq. (2.1) is expanded as

$$\begin{aligned}
 & \int_0^{x_0} \left[\frac{\partial E}{\partial h} + p_c - \frac{\sigma h_{xx}}{(1+h_x^2)^{3/2}} - \frac{d}{dx} \left(\frac{\partial E}{\partial h_x} \right) \right] \delta h dx - \left[\frac{\sigma h_x}{(1+h_x^2)^{1/2}} - \frac{\partial E}{\partial h_x} \right] \delta h \Bigg|_{x=0} \\
 & + \left[\frac{\sigma}{(1+h_x^2)^{1/2}} + \sigma_{fs} - \sigma_{sg} + E - h_x \frac{\partial E}{\partial h_x} \right]_{x=x_0} \delta x_0 = 0,
 \end{aligned} \tag{2.2}$$

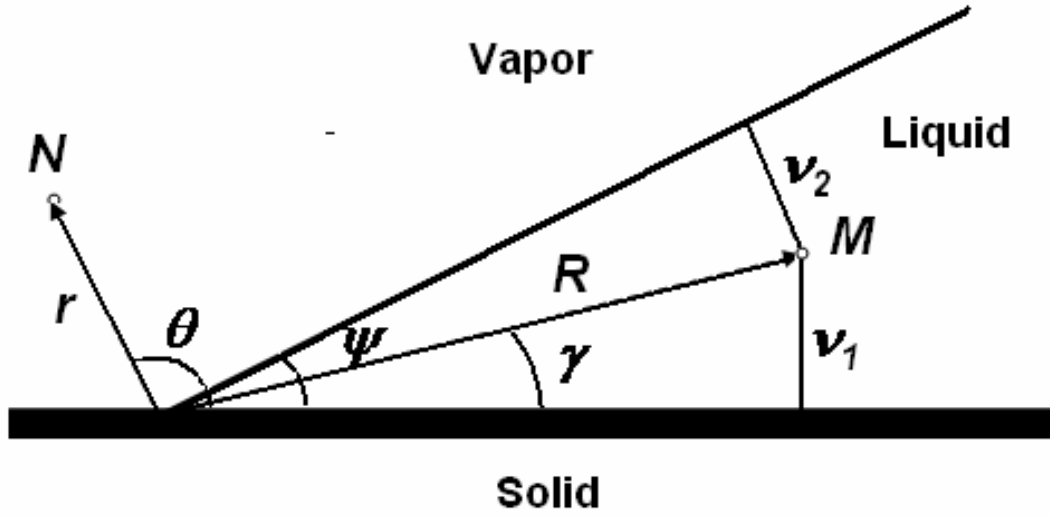


Figure 2.2 A wedge liquid film is located near a solid substrate in the cylindrical coordinate where the wedge slope is ψ . Position of the liquid molecule M is (R, γ, θ) and the other arbitrary molecule N is located at (r, θ, z) where $-\infty < z < \infty$. Parameters ν_1 and ν_2 are the shortest distance from position M to the solid surface and the wedge interface.

where $\delta h|_{x=x_0} = -h_x \delta x_0|_{x=x_0}$.

All terms inside the brackets in Eq. (2.2) must be zero because δh and δx_0 are arbitrary.

The first term leads to the augmented Young-Laplace equation:

$$-\frac{\partial E}{\partial h} + \frac{\sigma h_{xx}}{(1+h_x^2)^{3/2}} + \frac{d}{dx} \left(\frac{\partial E}{\partial h_x} \right) = p_c. \quad (2.3)$$

The second and third terms in Eq. (2.2) give boundary conditions at the center of the drop and the end of the drop. This equation reduces to that of Yeh et al. (1999) if $E = E(h)$ only. A disjoining pressure can be defined by comparing with the regular augmented Young-Laplace

equation as

$$\Pi = -\frac{\partial E}{\partial h} + \frac{d}{dx} \left(\frac{\partial E}{\partial h_x} \right). \quad (2.4)$$

To find the excess energy E , an intermolecular potential model must be selected and the Lennard-Jones intermolecular potential is used. Figure 2.2 shows a liquid wedge on a solid substrate. This figure uses the cylindrical coordinate (r, θ, z) and the contact angle ψ is constant.

The Lennard-Jones potential ϕ is

$$\phi_{fs} = \frac{\nu_{fs}}{MN^{12}} - \frac{\beta_{fs}}{MN^6}, \phi_{ff} = \frac{\nu_{ff}}{MN^{12}} - \frac{\beta_{ff}}{MN^6}, \phi_{fg} = \frac{\nu_{fg}}{MN^{12}} - \frac{\beta_{fg}}{MN^6}, \quad (2.5)$$

where ν is the strength of the repulsive potential, β is the strength of the attractive potential.

Subscripts fs , ff , and fg denote liquid-solid, liquid-liquid, and liquid-vapor states. In fact, Wu and Wong (2004) published similar results by using the van der Waals potential. Here, I focus on the repulsive potential terms.

By summing the potential between liquid molecule M and other molecules, the total intermolecular potential per unit volume at M is shown in Appendix A

$$\Phi_{total} = -\frac{\pi n_f^2 \nu_{ff}}{11520} \left(\frac{b_1(1-\zeta) + 256(\zeta - \varphi)}{v_1^9} + \frac{b_2(1-\zeta)}{v_2^9} \right) + \frac{\pi n_f^2 \beta_{ff}}{6} \left(\frac{a_1(1-\rho) + \rho - \lambda}{v_1^3} + \frac{a_2(1-\rho)}{v_2^3} \right), \quad (2.6)$$

where $v_1 (= R \sin \gamma)$ is the height of the molecule in the liquid from the solid substrate, $v_2 (= R \sin(\psi - \gamma))$ is the distance between a liquid molecule and the liquid surface, and n_f is the

number density of the liquid molecules. In addition, other parameters are defined as

$$\begin{aligned}\varphi &= \frac{n_s \nu_{fs}}{n_f \nu_{ff}} \quad , \quad \zeta = \frac{n_g \nu_{fg}}{n_f \nu_{ff}} \quad , \quad \lambda = \frac{n_s \beta_{fs}}{n_f \beta_{ff}} \quad , \quad \rho = \frac{n_g \beta_{fg}}{n_f \beta_{ff}} \quad , \\ a_1 &= \frac{1}{2} + \frac{3}{4} \cos \gamma - \frac{1}{4} \cos^3 \gamma \quad , \\ a_2 &= \frac{1}{2} + \frac{3}{4} \cos(\psi - \gamma) - \frac{1}{4} \cos^3(\psi - \gamma) \quad , \\ b_1 &= 128 + 315 \cos \gamma - 420 \cos^3 \gamma + 378 \cos^5 \gamma - 180 \cos^7 \gamma + 35 \cos^9 \gamma \quad , \\ b_2 &= 128 + 315 \cos(\psi - \gamma) - 420 \cos^3(\psi - \gamma) + 378 \cos^5(\psi - \gamma) \\ &\quad - 180 \cos^7(\psi - \gamma) + 35 \cos^9(\psi - \gamma) \quad .\end{aligned}\tag{2.7}$$

Excess energy E is defined as

$$E = \int_D^h (\Phi_{total} - \Phi_{\infty}) dy \quad .\tag{2.8}$$

Here, Φ_{∞} is the bulk component of Φ as the height of M diverge to infinite. The bulk component must be subtracted from the total intermolecular potential Φ_{total} because Φ_{total} includes both thin-film component and the bulk component and because E is an interaction energy due only to thin-film forces. The value of E is evaluated in the limit $h_x \rightarrow 0$ to yield (Appendix B)

$$E = \frac{7\pi n_f^2 \nu_{ff}}{40h^8} \left(\frac{1-\varphi}{63} + \frac{1-\zeta}{64} h_x^{10} \right) - \frac{\pi n_f^2 \beta_{ff}}{4h^2} \left(\frac{1-\lambda}{3} + \frac{1-\rho}{8} h_x^4 \right) \quad .\tag{2.9}$$

Following equation (2.4), a disjoining pressure is expressed as

$$\Pi = \frac{T}{h^9} \left(\eta^{10} - h_x^{10} + \frac{5}{4} h h_x^8 h_{xx} \right) - \frac{S}{h^3} \left(\alpha^4 - h_x^4 + 2h h_x^2 h_{xx} \right) \quad ,\tag{2.10}$$

$$\text{where } T = \frac{63\pi n_f^2 \nu_{ff} (1-\zeta)}{320} \quad , \quad S = \frac{3\pi n_f^2 \beta_{ff} (1-\rho)}{16} \quad ,\tag{2.11}$$

$$\eta = \left(\frac{64(1-\varphi)}{567(1-\zeta)} \right)^{\frac{1}{10}} \quad , \quad \alpha = \left(\frac{8(1-\lambda)}{9(1-\rho)} \right)^{\frac{1}{4}} \quad .$$

This disjoining pressure includes a repulsive component as well as the attractive component

derived earlier (Wu and Wong 2004). It also allows a liquid drop on a solid surface to have two angles in the partial wetting case: a macroscopic contact angle (α) and a microscopic contact angle at the film edge (η).

CHAPTER 3. BOUNDARY CONDITIONS

Two boundary conditions in Eq. (2.2) are imposed at $x=0$ and $x = x_0$. The boundary condition at $x=0$ lead to

$$\frac{2h_x}{(1+h_x^2)^{1/2}} - \frac{7\pi m_f^2 \nu_{ff}(1-\zeta)h_x^9}{256h^8} - \frac{\pi m_f^2 \beta_{ff}(1-\rho)h_x^3}{4h^8} = 0. \quad (3.1)$$

This boundary condition implies $h_x = 0$. The second condition at $x \rightarrow x_0$ is

$$\left. \frac{\sigma}{(1+h_x^2)^{1/2}} + \sigma_{fs} - \sigma_{sg} + E - h_x \frac{\partial E}{\partial h_x} \right|_{x=x_0} = 0 \quad (3.2)$$

Form Eq. (2.9),

$$E - h_x \frac{\partial E}{\partial h_x} = \frac{T}{8} \left(\frac{\eta^{10} - h_x^{10}}{h^8} \right) - \frac{S}{2} \left(\frac{\alpha^4 - h_x^4}{h^2} \right). \quad (3.3)$$

Far from the precursor film, the repulsive term is weak, and we recover the case studied by Wu and Wong (2004), in which

$$h_x \rightarrow \alpha, \quad (3.4)$$

near the macroscopic contact line. Thus, α is the macroscopic contact angle at the macroscopic (apparent) contact line. For the augmented Young-Laplace equation to be well behaved as $h \rightarrow 0$, we need (Appendix G.3).

$$|h_x| \rightarrow \eta, h^{(2)} = h^{(3)} = h^{(4)} = h^{(5)} = h^{(6)} = h^{(8)} = 0, h^{(7)} \rightarrow \frac{288S(\eta^4 - \alpha^4)}{\eta^3 T}, \quad (3.5)$$

where $h^{(n)} \equiv \partial^n h / \partial x^n$. When these conditions are imposed in Eq. (3.3), we find as $h \rightarrow 0$,

$$E - h_x \frac{\partial E}{\partial h_x} \rightarrow 0.$$

$$\frac{\sigma}{(1 + h_x^2)^{1/2}} + \sigma_{fs} - \sigma_{sg} \rightarrow 0.$$

Thus, the Young equation holds near the microscopic contact line.

CHAPTER 4. AUGMENTED YOUNG-LAPLACE EQUATION

From Eq. (2.3), the augmented Young-Laplace equation is

$$p_c = \sigma h_{xx} + \frac{T}{h^9} \left(\eta^{10} - h_x^{10} + \frac{5}{4} h h_x^8 h_{xx} \right) - \frac{S}{h^3} \left(\alpha^4 - h_x^4 + 2h h_x^2 h_{xx} \right) \quad (4.1)$$

The pressure difference $p_c = p_f - p_g$ is equal to the capillary pressure plus the repulsive component of the disjoining pressure plus the attractive component. There are two contact angles: microscopic η and macroscopic α . Both the macroscopic and microscopic contact angles are affected by intermolecular forces.

The governing equation is non-dimensionalized. Let $H = h/h_0$, $X = \alpha x/h_0$ (where h_0 is an unspecified film thickness), then

$$C = H_{XX} + R \left(\frac{\xi^{10} - H_X^{10} + \frac{5}{4} H H_X^8 H_{XX}}{H^9} \right) - \varepsilon \left(\frac{1 - H_X^4 + 2H H_X^2 H_{XX}}{H^3} \right), \quad (4.2)$$

$$\varepsilon = \frac{S\alpha^2}{\sigma h_0^2}, R = \frac{T\alpha^8}{\sigma h_0^8}, \xi^{10} = \left(\frac{\eta}{\alpha} \right)^{10}, C = \frac{p_c h_0}{\sigma \alpha^2}, \quad (4.3)$$

where C is a non-dimensionalized pressure difference, ε and R are strengths of van der Waals and repulsive potential components non-dimensionalized by surface tension, and ξ is the ratio of nanoscopic contact angle to the macroscopic contact angle of the main drop.

It is possible to integrate Eq. (4.2) with respect to H as

$$\frac{1}{2}H_x^2 + \varepsilon \left(\frac{1 - H_x^4}{2H^2} \right) - R \left(\frac{\xi^{10} - H_x^{10}}{8H^8} \right) = CH + K, \quad (4.4)$$

where K is a constant of integration. This equation is needed for determining the precursor film thickness.

Next chapter will show how to find uniform film thicknesses.

CHAPTER 5. UNIFORM FILM SOLUTIONS

Two uniform film solutions have been found from the augmented Young-Laplace equation.

These two cases satisfy the same conditions: zero slope and zero curvature. By substituting these two conditions into Eq. (2.11), we find

$$C = -\varepsilon \left(\frac{1}{H^3} \right) + R \left(\frac{\xi^{10}}{H^9} \right), \quad (5.1)$$

where H is the uniform film thickness. The parameters ε , R , and ξ all depends on the molecular potential of the liquid drop, and are fixed for a specific liquid. The parameter C , however, is the dimensionless pressure difference and can be varied. For a given value of C , there are nine solutions of the film thickness H . Six are complex and three are real as shown in Appendix D.

Another relation between C and H comes from the integrated Eq. (4.2). By imposing the boundary condition at the center of the drop: $H = 1$ and $H_x = 0$, we find the integration constant K as

$$K = -C + \frac{\varepsilon}{2} - \frac{R\xi^{10}}{8}. \quad (5.2)$$

Thus, the integrated equation with $H_x = 0$ becomes

$$C = -\frac{\varepsilon(1+H)}{2H^2} + \frac{R\xi^{10}(1+H)(1+H^2)(1+H^4)}{8H^8}. \quad (5.3)$$

By eliminating C between Eq. (5.1) and (5.3), we get

$$(H-1) \left\{ -\frac{(H+2)}{2H^2} + \left(\frac{R\xi^{10}}{\varepsilon} \right) \frac{(8+7H+6H^2+5H^3+4H^4+3H^5+2H^6+H^7)}{8H^8} \right\} = 0. \quad (5.4)$$

This equation has two real and positive solutions: $H=1$ and $H = H_p = H_p(R\xi^{10}/\varepsilon)$. Other solutions are either complex or negative for $R\xi^{10}/\varepsilon \ll 1$.

If $H=1$, then Eq. (5.1) gives

$$C = C_1 = -\varepsilon + R\xi^{10}. \quad (5.5)$$

If $H = H_p$, then Eq. (5.1) shows

$$C = C_2 = -\frac{\varepsilon}{H_p^3} + \frac{R\xi^{10}}{H_p^9}. \quad (5.6)$$

As shown in chapter 5, these two values C_1 and C_2 separate the drop shapes into seven groups:

$C < C_2, C = C_2 - \delta, C = C_2, C = C_2 + \delta, C_2 - \delta < C < C_1, C = C_1,$ and $C_1 < C$, where δ is a small positive number.

No analytic expression is found for H_p . However, a numerical solution can always be calculated for any given value of $R\xi^{10}/\varepsilon$. Results of $H_p = H_p(R\xi^{10}/\varepsilon)$ are plotted in Fig. 5.1.

Since the precursor film thickness H_p depends only on $R\xi^{10}/\varepsilon$, it is important to estimate the value of $R\xi^{10}/\varepsilon$. Consider another form of the Lennard-Jones potential:

$$\phi(r) = 4e \left[\left(\frac{r_0}{r} \right)^{12} - \left(\frac{r_0}{r} \right)^6 \right], \quad (5.7)$$

where e is the well depth and r_0 is the collision diameter. By comparing with Eq. (2.5), we find

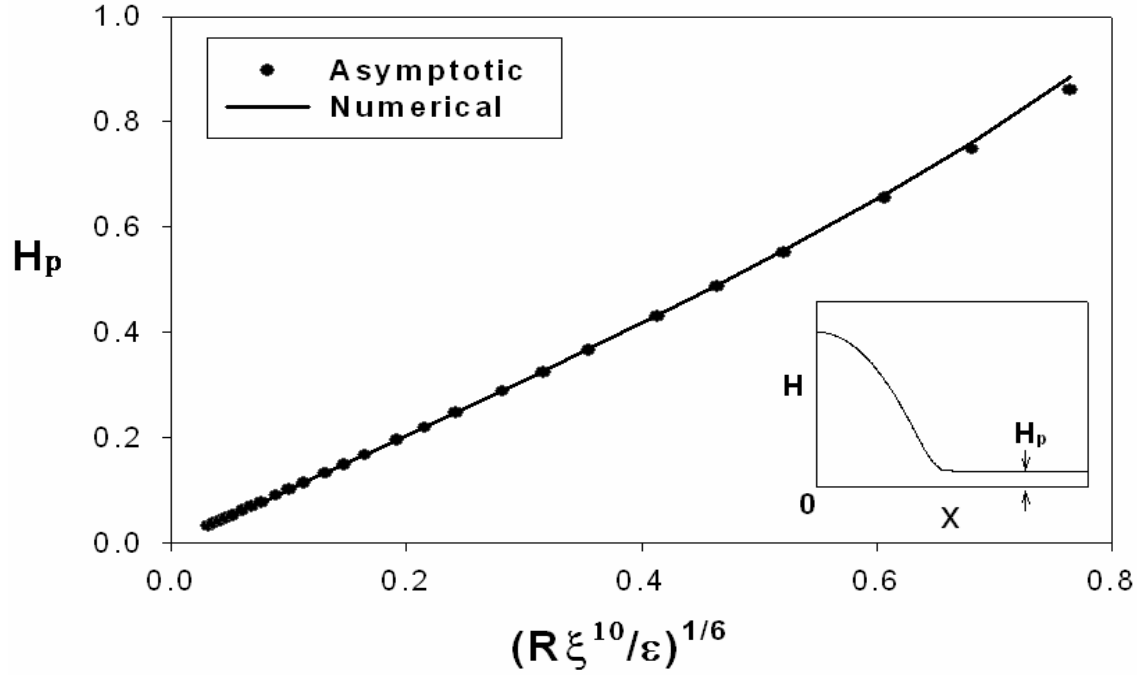


Figure 5.1 Numerical solutions versus asymptotic solutions for the precursor film thickness H_p . This figure shows that the precursor film thickness is proportional to $(R\xi^{10}/\epsilon)^{1/6}$ when $R\xi^{10}/\epsilon \ll 1$.

$\nu = 4er_0^{12}$ and $\beta = 4er_0^6$. Following the definition of ϵ , R , and ξ in Eqs. (2.11) and (4.3), the ratio is given by

$$\frac{R\xi^{10}}{\epsilon} = \frac{2(n_f \nu_{ff}^{12} - n_s \nu_{fs}^{12})}{15(n_f \beta_{ff}^6 - n_s \beta_{fs}^6)h_0^6} = \frac{2(n_f e_{ff} r_{0ff}^{12} - n_s e_{sf} r_{0fs}^{12})}{15(n_f e_{ff} r_{0ff}^6 - n_s e_{sf} r_{0fs}^6)h_0^6}. \quad (5.8)$$

If we take $r_{0ff} = r_{0fs} = r_0$, then

$$\frac{R\xi^{10}}{\epsilon} = \frac{2}{15} \left(\frac{r_0}{h_0} \right)^6. \quad (5.9)$$

Since $h_0 > r_0$, the ratio $R\xi^{10}/\epsilon \ll 1$.

An asymptotic solution is derived for H_p in the limit $R\xi^{10}/\varepsilon \rightarrow 0$ as shown in Appendix E:

$$H_p = \delta' + \frac{1}{24}\delta'^2 + \frac{29}{288}\delta'^3 + \frac{3415}{82944}\delta'^4 + \frac{36353}{1327104}\delta'^5 + \frac{4014713}{191102976}\delta'^6 + O(\delta'^7), \quad (5.10)$$

where $\delta' = (R\xi^{10}/\varepsilon)^{\frac{1}{6}}$. This is also plotted in Fig. 5.1. and agrees well with the numerical solution for $\delta' \ll 1$.

CHAPTER 6. EQUILIBRIUM DROPS PROFILES

The augmented Young-Laplace equation includes four parameters: C , ε , R , and ξ . Thus, the drop shape depends on the values of C , ε , R and ξ . In this chapter, the effects of these parameters will be studied systematically.

Figure 6.1 shows various profiles of the liquid drop on a solid substrate for different C , with ε , R and ξ fixed.

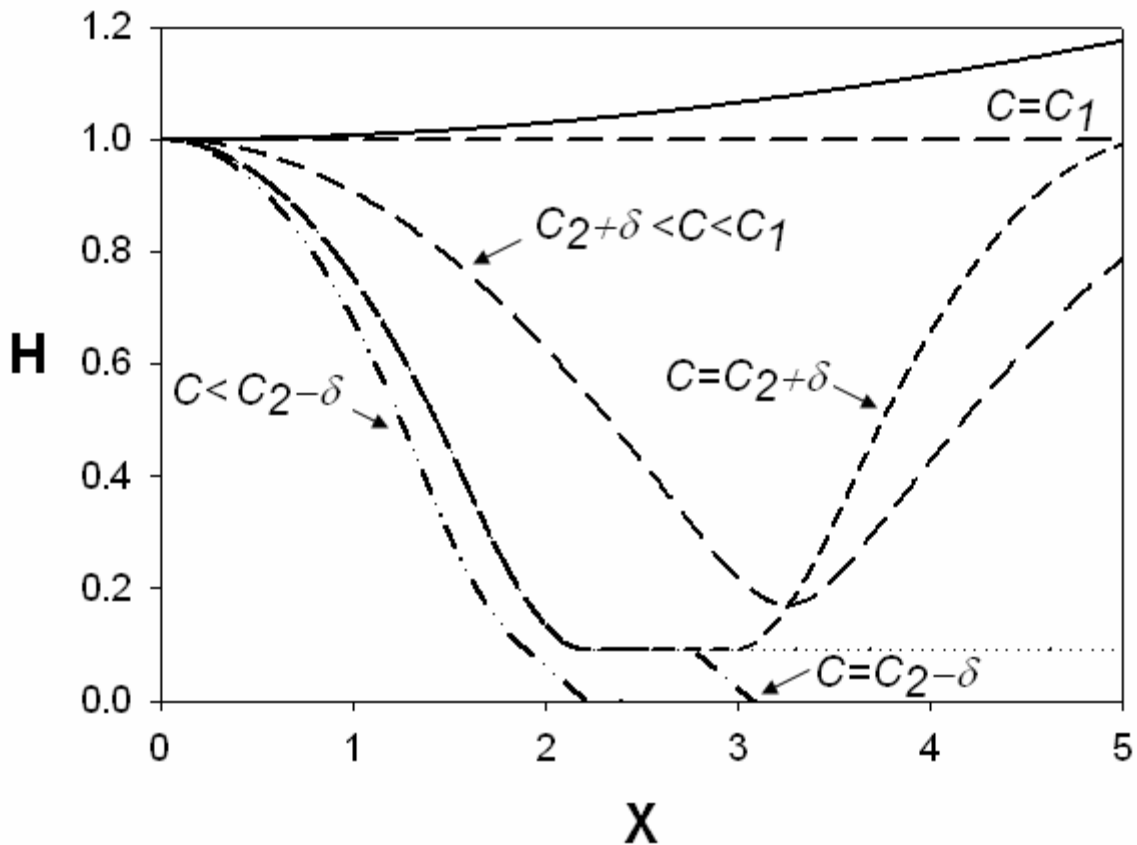


Figure 6.1 Depending on the parameter C , the drop profile can be divided into seven groups. In the legend, C_1 and C_2 are critical values for the uniform film and pseudo partial wetting drop cases, and δ is a small positive number. Here, $(\varepsilon, R, \xi) = (0.01, 5.43 \times 10^{-9}, 1)$.

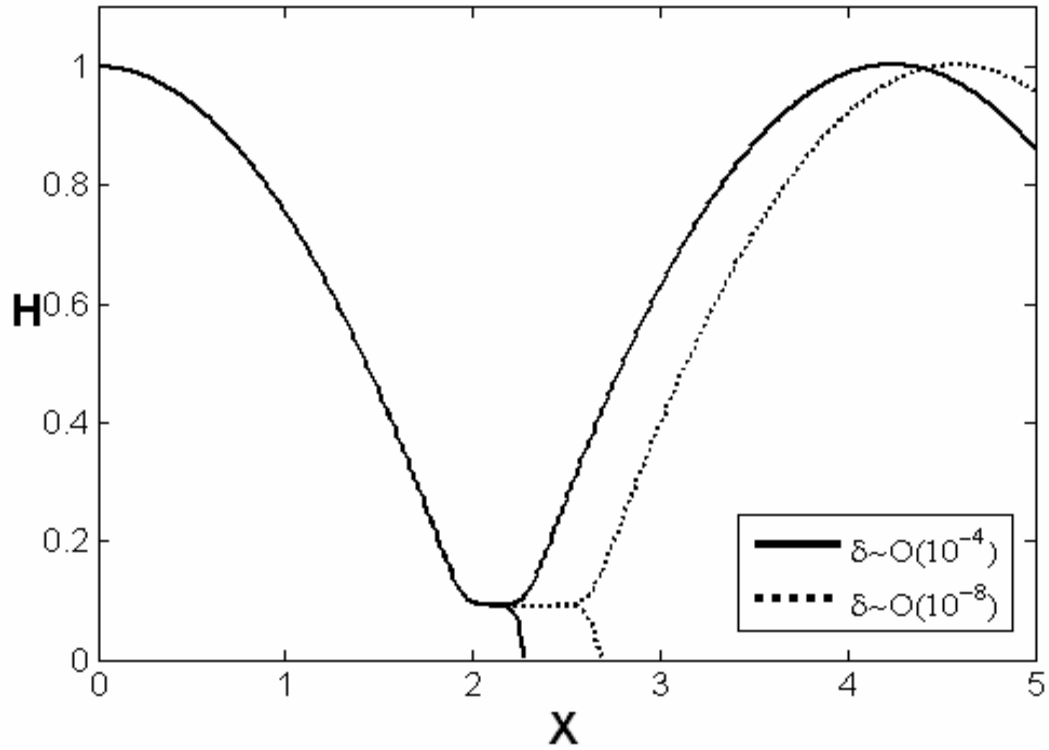


Figure 6.2 Effect of δ on the drop profile. Here, $(C, \varepsilon, R, \xi) = (C_2 \pm \delta, 0.01, 5.43 \times 10^{-9}, 1.0)$ when C is close to C_2 . Depending on the value of C , the length of the precursor film varies.

The reason for C to be selected as a control variable is that the pressure difference is controllable and the other parameters are characteristics of the material. The profile is calculated by solving the augmented Young-Laplace equation (4.2) numerically using a Runge-Kutta scheme. This step size used in the integration is 10^{-2} and the accuracy of this scheme is $O(10^{-8})$. At the center of the drop, $H=1$ and $H_X=0$. This is sufficient to start the integration.

The previous chapter shows two C values: C_1 and C_2 . When $C=C_1$, the non-dimensional film height $H=1$. If $C>C_1$, then the film height increases and becomes unbounded. When $C=C_2$, the

drop has an unbounded precursor film (see Appendix F). If $C = C_2 + \delta$, where δ is a small positive number, then the precursor film height starts to increase at some point and another drop is formed. As δ decreases, the precursor film lengthens, as shown in Fig. 6.2. If $C = C_2 - \delta$, then the precursor film ends at the substrate. The length of the film again depends on δ as illustrated in Fig. 6.2.

If $C_2 + \delta < C < C_1$, then the drop is attached to another drop without the intermediate precursor film (Fig.6.1). The two drops are identical.

If $C < C_2 - \delta$, then the drop ends at the substrate without a precursor film, but the slope changes from unity to ξ near the end.

Figure 6.3 demonstrates how the precursor film profile changes with intermolecular parameters ε and R . If R increases and ε is fixed, the curvature of the drop would decrease and the thickness of the precursor film increases. In contrast, if ε increases and R is fixed, the drop is more pointed and the precursor film thickness decreases.

Figure 6.4 shows that if the ratio $R\xi^{10}/\varepsilon$ is held constant, the thickness does not change. As shown by the asymptotic solution Eq. (5.10), $H_p \rightarrow R\xi^{10}/\varepsilon$ as $R\xi^{10}/\varepsilon \rightarrow 0$.

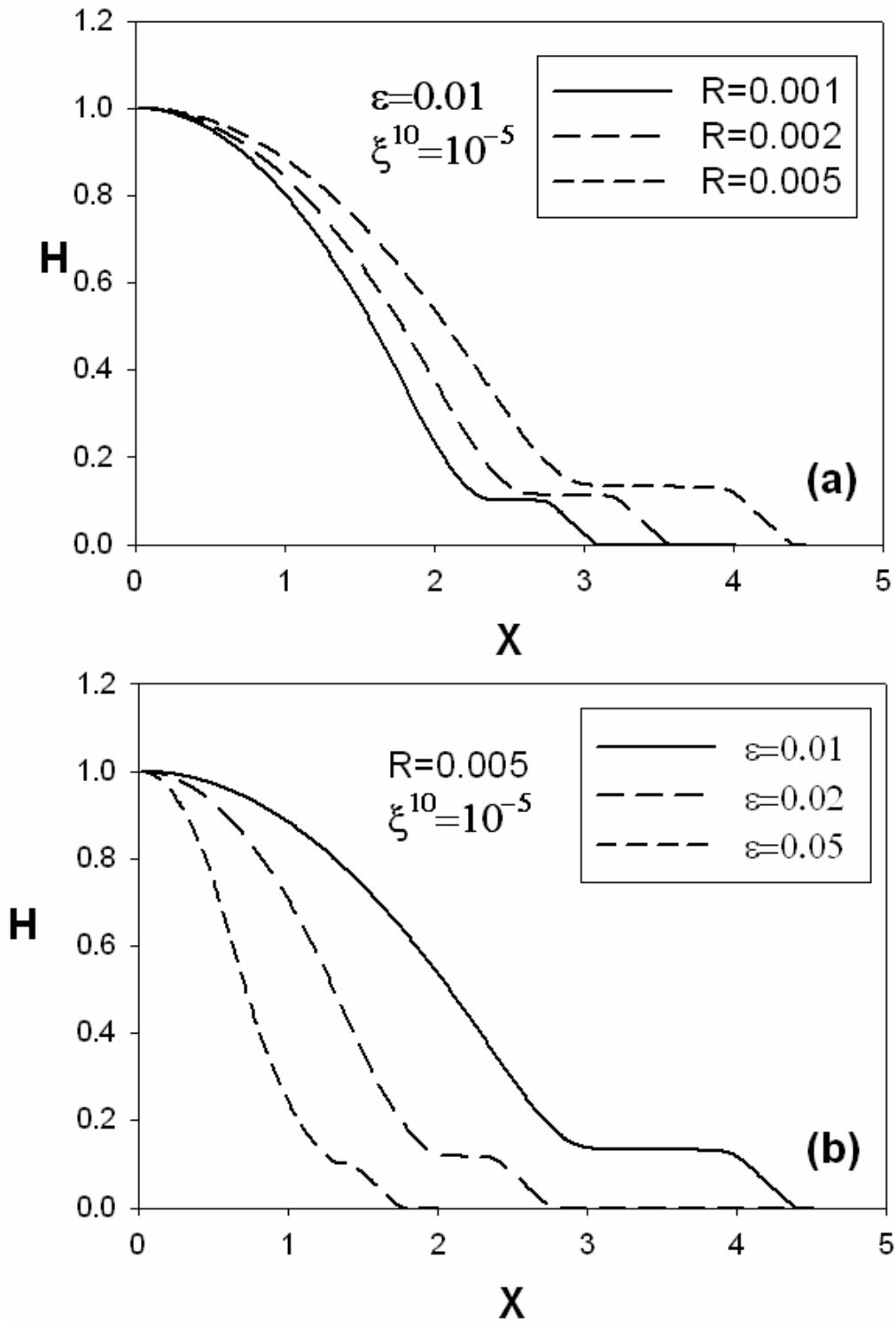


Figure 6.3 Pseudo partial wetting drop profiles for different ε and R . The pressure difference $C = C_2 - \delta$ where $\delta \sim O(10^{-3})$ and C_2 depends on ε , R and ξ . Here, C_2 values were calculated by substituting Eq. (5.10) into Eq. (5.6).

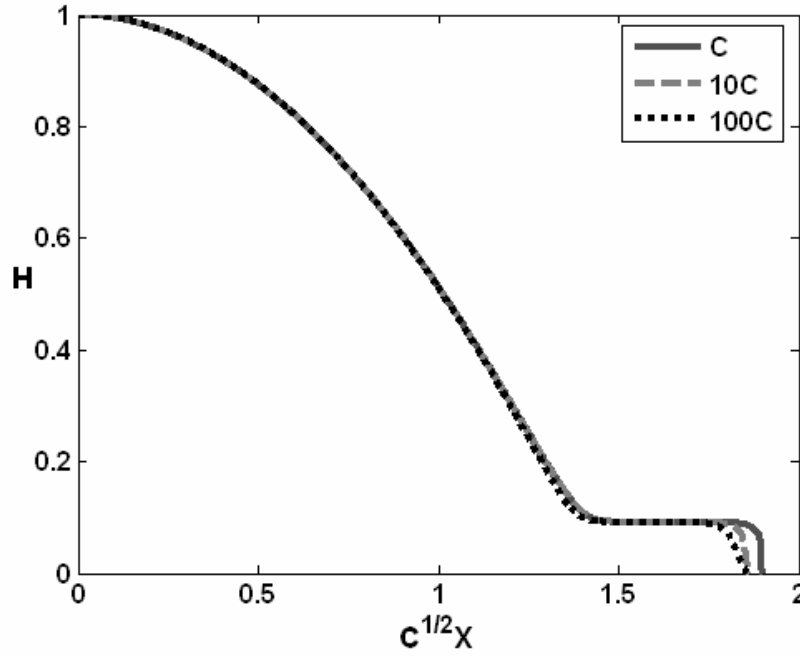


Figure 6.4 Film profiles for fixed $R\xi^{10}/\varepsilon$ for $C_2 - \delta$ cases. In this figure, data set of $(C, \varepsilon, R\xi^{10})$ used is $(-0.5, 0.01, 0.0000000543)$. Here, when C is increased by 10 times, ε and $R\xi^{10}$ are also increased by the same proportion.

Another interesting case is the periodic profiles in Fig. 6.1. The third line looks like periodic waves. Fig. 6.5 and 6.6 show the period and the area over one period versus C for $C_2 < C < C_1$. As shown in these two figures, both period and area would diverge to infinity near the two critical values C_1 and C_2 . Physically, this phenomenon is reasonable because a drop near $C=C_1$ or $C=C_2$ contains an infinite uniform film or endless precursor film (i.e. there is no period). These fluctuating profiles have been observed in molecular-dynamics simulations (Sharma and Verma 2004, Xie et al. 1998).

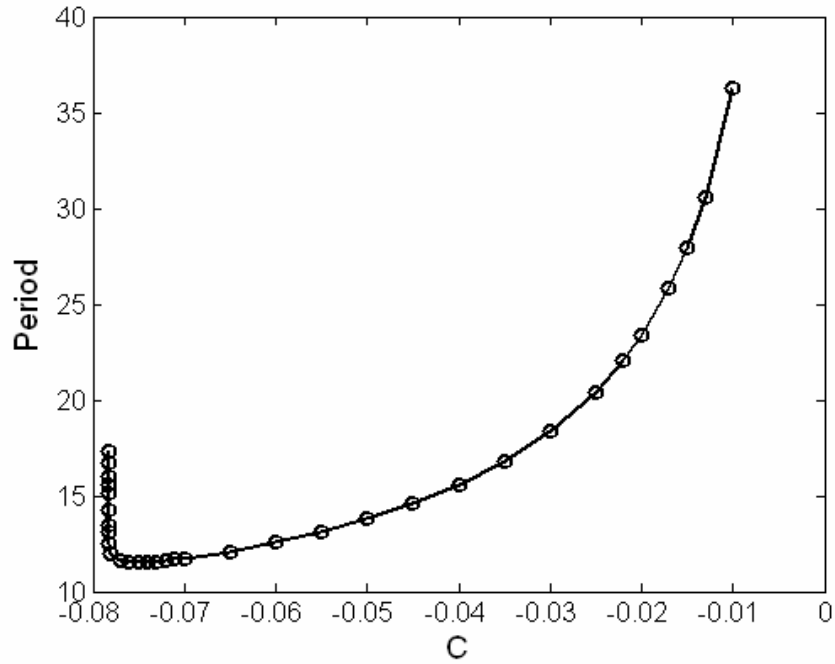


Figure 6.5 Period versus C for drops connected by a thin-film for fixed intermolecular potential parameters $(\varepsilon, R\xi^{10})$. If C approaches the critical values (C_1, C_2) , the period will diverge.

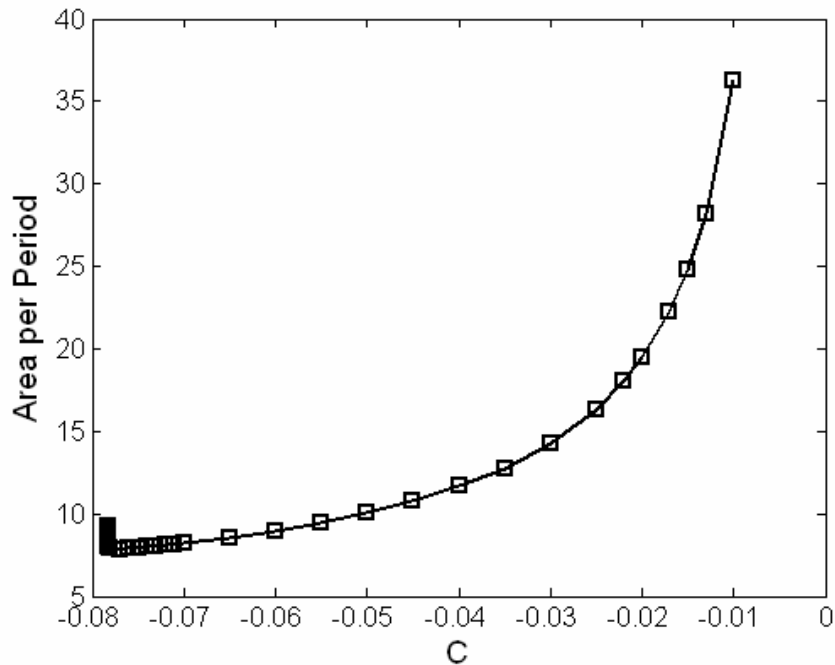


Figure 6.6 Area per period versus C for drops connected by a thin-film for fixed $(\varepsilon, R\xi^{10})$. The area has the similar property as the period in Fig. 6.5. If C approaches a critical value, the area will be infinite.

CHAPTER 7. STABILITY ANALYSIS OF UNIFORM FILMS

The evolution of a thin-film with small slopes obeys (Oron et al. (1997))

$$\frac{\partial h}{\partial t} - \frac{1}{3\mu} \frac{\partial}{\partial x} \left[h^3 \frac{\partial p_f}{\partial x} \right] = 0, \quad (7.1)$$

where t is time and μ is viscosity. The liquid pressure (p_f) is formed by the augmented Young-Laplace equation as

$$p_f = p_g - \sigma h_{xx} - \Pi, \quad (7.2)$$

where σ is the liquid-vapor surface tension, p_g is the vapor pressure, and Π is the disjoining pressure. Because the slope of the film is assumed small, the curvature in the capillary pressure term is h_{xx} . This incurs an error of $O(h_x^2)$.

The evolution equation can be made dimensionless by defining

$$H = \frac{h}{h_0}, X = \frac{\alpha x}{h_0}, \tau = \frac{t\sigma\alpha^4}{\mu h_0}. \quad (7.3)$$

Eq. (7.1) is transformed into

$$\frac{\partial H}{\partial \tau} + \frac{1}{3} \frac{\partial}{\partial X} \left[H^3 \frac{\partial}{\partial X} \left(H_{XX} - \frac{\varepsilon \left(1 - H_X^4 + 2HH_X^2 H_{XX} \right)}{H^3} + \frac{R\xi^{10} \left(1 - H_X^{10} + \frac{5}{4} HH_X^8 H_{XX} \right)}{H^9} \right) \right] = 0 \quad (7.4)$$

This equation admits a uniform film $H=1$ as a solution. The uniform film is perturbed by a small disturbance δ :

$$H(\tau, X) = 1 + \delta(\tau, X). \quad (7.5)$$

Eq. (7.4) then becomes

$$\delta_\tau + \frac{1}{3}\delta_{XXXX} + (\varepsilon - 3R\xi^{10})\delta_{XX} = 0. \quad (7.6)$$

In Eq. (7.6), $(\varepsilon - 3R\xi^{10})$ is positive (See Appendix F). The leading order equation is linear in

δ and amenable to a normal mode analysis:

$$\delta(\tau, X) = e^{\omega\tau} f(X). \quad (7.7)$$

where ω is the growth rate and f is the eigenfunction. Eq. (7.7) is substituted into Eq. (7.6):

$$\frac{1}{3}f'''' + (\varepsilon - 3R\xi^{10})f'' + \omega f = 0. \quad (7.8)$$

Since this equation is linear in f , it admits a solution of the form $f = e^{ikX}$. This gives the growth rate as

$$\omega = -\frac{1}{3}k^2 \left[k^2 - (3\varepsilon - 9R\xi^{10}) \right]. \quad (7.9)$$

If $k \geq (3\varepsilon - 9R\xi^{10})^{\frac{1}{2}}$, the uniform film is stable; otherwise, it is unstable. Thus, long wave perturbations are unstable.

The above analysis can also be applied to the precursor film. A precursor film of thickness $H = H_p$ also satisfies Eq. (7.4). The uniform film is again perturbed by $H(\tau, X) = H_p + \delta(\tau, X)$.

The perturbation δ obeys

$$\delta_\tau + \frac{1}{3}H_p^3\delta_{XXXX} + \left(\frac{\varepsilon}{H_p} - \frac{3R\xi^{10}}{H_p^7} \right) \delta_{XX} = 0. \quad (7.8)$$

If $\delta(\tau, X) = e^{\omega\tau} f(X)$, then

$$f'''' + \left(\frac{3\varepsilon}{H_p^4} - \frac{9R\xi^{10}}{H_p^{10}} \right) f'' + \frac{3\omega}{H_p^3} f = 0. \quad (7.9)$$

We take $f = e^{ikX}$, then

$$\omega = -\frac{1}{3}k^2 H_p^3 \left[k^2 - \left(\frac{3\varepsilon}{H_p^4} - \frac{9R\xi^{10}}{H_p^{10}} \right) \right]. \quad (7.10)$$

From Eq. (5.10), $H_p = (R\xi^{10}/\varepsilon)^{1/6} + (R\xi^{10}/\varepsilon)^{1/3}/24 + \dots$. Using this relation,

$$\left(\frac{3\varepsilon}{H_p^4} - \frac{9R\xi^{10}}{H_p^{10}} \right) = \frac{3\varepsilon}{H_p^4} \left(1 - \frac{3R\xi^{10}}{\varepsilon H_p^6} \right) = \frac{3\varepsilon}{H_p^4} \left[-2 + \frac{1}{4} \left(\frac{R\xi^{10}}{\varepsilon} \right)^{1/6} \right] < 0. \quad (7.11)$$

Thus, the precursor film is always stable.

CHAPTER 8. DISCUSSIONS AND CONCLUSIONS

This work derives a new disjoining pressure expression for Lennard-Jones thin-films. The expression contains a short-range repulsive term as well as the long-range attractive term derived by Wu and Wong (2004).

This disjoining pressure is incorporated into the augmented Young-Laplace equation, which governs the equilibrium drop and meniscus shapes. The governing equation is made dimensionless by the maximum height of the drop and four dimensionless numbers emerge: C , ε , R , and ξ . The parameter C is the dimensionless pressure difference between the vapor and liquid, and ε , R , and ξ depend on the intermolecular potential. Hence, C can be varied in an experimental set-up whereas ε , R , and ξ are fixed for a particular material system. We find two critical values of C : C_1 and C_2 . The value of $C_1 = C_1(\varepsilon, R, \xi)$ corresponds to a uniform film of unit height. The value $C_2 = C_2(\varepsilon, R, \xi)$ yields a drop with a precursor film that extends to infinity.

We find that if $C > C_1$, then the film height $H \sim X^2$ as $X \rightarrow \infty$. If $C_2 < C < C_1$, then the drop height is a periodic function of X implying an array of drops. If $C < C_2$, then the precursor film terminates at the substrate.

We also study the linear stability of uniform films and find that the film with unit height is unstable to long-wave perturbations, whereas the precursor film is unconditionally stable.

REFERENCES

S.G. Ash, D.H. Everett and C.J. Radke, "Thermodynamics of adsorption forces," J. Chem. Soc.-Far Trans II, **69**, 1256 (1973).

C.M. Bender and S.A. Orszag, *Advanced Mathematical Methods for Scientists and Engineers*, Springer Chap VII (1999)

V. Bergeron, "Forces and Structure in thin liquid Soap films," J. Phys.: Condens. Matter **11**, R215 (1999)

D. Bonn et al., "Complex wetting phenomena in liquid mixtures: frustrated-complete wetting and competing intermolecular forces," J. Phys.: Condens. Matter **13**, 4903 (2001)

F. Brochard-Wyart, "Spreading of Nonvolatile Liquids in a Continuum Picture," Langmuir **7**, 335 (1991)

H.J. Butt, K. Graf, and M. Kappl, *Physics and Chemistry of Interfaces*, WILEY-VCH Chap 3,4,6,7 (2003)

R. Courant and D. Hilbert, *METHODS OF MATHEMATICAL PHYSICS*, Interscience Chap. 4 (1953)

J.M.Davis and S.M.Troian, "Influence of attractive van der Waals interactions on the optimal excitations in thermocapillary-driven spreading," Phys. Rev. E **67**, 016308 (2003)

P.G. de Gennes, F. Brochard-Wyart, D. Quere, *Capillarity and Wetting Phenomena: Drops Bubbles, Pearls, Waves*, Springer Chap 4 (2003)

B.V. Derjaguin, A.S. Titijevskaya, in: J.H. Schulman (Ed.), Proc. 2nd Int. Congr. Surface Activity, vol. **1**, Butterworths 211 (1957)

S.J. Gokhale, S. DasGupta, J. L. Plawsky, and P. C. Wayner, Jr., "Reflectivity-based evaluation of the coalescence of two condensing drops and shape evolution of the coalesced drop," Phys. Rev.

E **70**, 051610 (2004)

L.M. Hocking., “The influence of intermolecular forces on thin fluid layers,” *Phys Fluids A* **5**, 793 (1993)

J. Israelachvili, *Intermolecular & Surface Forces* 2nd ed. 9th printing, Academic Press Chap 10 (2002)

C. Kittel and H. Kroemer, *Thermal Physics* 7th ed. , W.H. Freeman and Company Chap 3 (1980)

C.A. Miller and E. Ruckenstein, “The Origin of Flow during Wetting of Solids,” *J.Colloid Sci.* **48**, 368 (1974)

J. Moon, S. Garoff, P. Wynblatt, and R. Suter, “Pseudopartial Wetting and Precursor Film Growth in Immiscible Metal Systems,” *Langmuir* **20**, 402 (2004)

P.M. Morse and H. Feshbach, *Methods of Theoretical Physics*, McGraw-Hill Science Chap. 9 (1953)

A. Oron, S.H. Davis, and S.G. Bankoff, “Long-scale evolution of thin liquid films,” *Rev. Mod. Phys.* **69**, 931-980 (1997)

G. Reiter et al., “Thin-film Instability Induced by Long-Range Forces,” *Langmuir* **15**, 2551 (1999)

P. Silberzan and L. Leger, “Evidence for a New Spreading Regime between Partial and Total Wetting,” *Phys. Rev. Let.* **66**, 185 (1991)

C. Stubenrauch and R. Klitzing, “Disjoining pressure isotherms of thin liquid films - new concepts and perspectives,” *J. Phys.: Condens. Matter* **15**, R1197 (2003)

L. Verlet and J.J. Weis, “Equilibrium Theory of Simple Liquids,” *Phys Rev. A* **5**, 939 (1972)

J.D. Weeks, D. Chandler and H.C. Andersen , “Role of Repulsive Forces in Forming the Equilibrium Structure of Simple Liquids,” *J. Chem. Phys.* **54**, 5237 (1971)

Q. Wu and H. Wong, "A slope-dependent disjoining pressure for non-zero contact angles," *J. Fluid Mechanics* **506**, 157 (2004)

E.K.Yeh, J. Newman, and C.J.Radke, "Equilibrium configurations of liquid droplets on solid surfaces under the influence of thin-film forces Part I. Thermo dynamics," *Colloids Surf. A* **156**, 136 (1999)

E.K.Yeh, J. Newman, and C.J.Radke, "Equilibrium configurations of liquid droplets on solid surfaces under the influence of thin-film forces Part II. Shape calculation," *Colloids Surf. A* **156**, 525 (1999)

APPENDIX A INTEGRATION OF THE INTERMOLECULAR POTENTIAL

Cylindrical coordinates(r, θ, z) are used here because the liquid film is a wedge(Fig. 2.2). As described in section 2, the molecules interact through the Lennard-Jones potential. The interactive potential between a liquid molecule and the solid substrate is

$$\Phi_{fs} = \iiint_{V_s} n_s \phi_{fs} dV = \int_{-\pi}^{\pi} \int_0^{\infty} \int_{-\infty}^{\infty} \frac{n_s \nu_{fs}}{MN^{12}} - \frac{n_s \beta_{fs}}{MN^6} r dz dr d\theta, \quad (\text{A.1})$$

where MN is the distance between the liquid molecule and a solid molecule, and $MN^2 = R^2 + r^2 + z^2 - 2rR \cos(\theta - \gamma)$, n_s is the number density of the solid molecules, ν_{fs} is the strength of the repulsive component, and β_{fs} is the strength of the attractive component.

Because the van der Waals potential part was already done by Wu and Wong (2004), I focus on the repulsive potential part. The basic procedure is the same as the previous research. Main application to calculate the intermolecular energy is Maple and Appendix H lists the program.

The integrals are evaluated by the following steps. The first step is the integration with respect to z :

$$\begin{aligned} & \int_{-\infty}^{\infty} \frac{1}{\{R^2 + r^2 + z^2 - 2rR \cos(\theta - \gamma)\}^6} dz \\ &= \int_{-\infty}^{\infty} \frac{1}{\{z^2 + MN^2\}^6} dz \end{aligned}$$

$$\begin{aligned}
&= \frac{1}{MN^{11}} \int_{-\frac{\pi}{2}}^{\frac{\pi}{2}} \cos^{10} \psi d\psi \\
&= \frac{1}{MN^{11}} \left[\sin \psi \cos \psi \left(\frac{1}{10} \cos^8 \psi + \frac{9}{80} \cos^6 \psi + \frac{21}{160} \cos^4 \psi + \frac{21}{128} \cos^2 \psi + \frac{62}{256} \right) + \frac{62}{256} \psi \right]_{-\frac{\pi}{2}}^{\frac{\pi}{2}} \\
&= \frac{63\pi}{256} \frac{1}{\{R^2 + r^2 - 2rR \cos(\theta - \gamma)\}^{1/2}}, \tag{A.2}
\end{aligned}$$

where $z = MN \tan \psi$ and $dz = (MN / \cos^2 \psi) d\psi$.

The integration with respect to r is performed as

$$\begin{aligned}
&\int_0^\infty \frac{1}{\{R^2 + r^2 - 2rR \cos(\theta - \gamma)\}^{1/2}} r dr \\
&= \int_0^\infty \frac{r - R \cos(\theta - \gamma)}{[\{r - R \cos(\theta - \gamma)\}^2 + R^2 \sin^2(\theta - \gamma)]^{1/2}} dr \\
&\quad + \int_0^\infty \frac{R \cos(\theta - \gamma)}{[\{r - R \cos(\theta - \gamma)\}^2 + R^2 \sin^2(\theta - \gamma)]^{1/2}} dr. \tag{A.3}
\end{aligned}$$

I split this equation into two parts and calculate each part separately.

$$\begin{aligned}
&\int_0^\infty \frac{r - R \cos(\theta - \gamma)}{[\{r - R \cos(\theta - \gamma)\}^2 + R^2 \sin^2(\theta - \gamma)]^{1/2}} dr \\
&= \int_0^\infty \frac{\frac{1}{2} d\{r - R \cos(\theta - \gamma)\}^2}{[\{r - R \cos(\theta - \gamma)\}^2 + R^2 \sin^2(\theta - \gamma)]^{1/2}} \\
&= -\frac{1}{9} \left([\{r - R \cos(\theta - \gamma)\}^2 + R^2 \sin^2(\theta - \gamma)]^{-1/2} \right)_0^\infty \\
&= \frac{1}{9R^9}. \tag{A.4}
\end{aligned}$$

$$\begin{aligned}
& \int_0^\infty \frac{R \cos(\theta - \gamma)}{[r - R \cos(\theta - \gamma)]^2 + R^2 \sin^2(\theta - \gamma)}^{1/2} dr \\
&= \frac{\cos(\theta - \gamma)}{R^9 \sin^{10}(\theta - \gamma)} \int_{\theta - \gamma - \frac{\pi}{2}}^{\frac{\pi}{2}} \cos^9 \varpi d\varpi \\
&= \frac{\cos(\theta - \gamma)}{R^9 \sin^{10}(\theta - \gamma)} \left[\frac{\sin \varpi \cos \varpi \left\{ \frac{1}{9} \cos^7 \varpi + \frac{8}{63} \cos^5 \varpi + \frac{128}{315} \sin \varpi \right\}}{\frac{16}{105} \cos^3 \varpi + \frac{64}{315} \cos \varpi} \right]_{\theta - \gamma - \frac{\pi}{2}}^{\frac{\pi}{2}} \\
&= \frac{\cos(\theta - \gamma)}{R^9 \sin^{10}(\theta - \gamma)} \left[\frac{128}{315} + \cos(\theta - \gamma) \left\{ \frac{1}{9} \sin^8(\theta - \gamma) + \frac{8}{63} \sin^6(\theta - \gamma) \right\} \right. \\
&\quad \left. + \frac{16}{105} \sin^4(\theta - \gamma) + \frac{64}{315} \sin^2(\theta - \gamma) + \frac{128}{315} \right]
\end{aligned} \tag{A.5}$$

where $r - R \cos(\theta - \gamma) = R \sin(\theta - \gamma) \tan \varpi$, $dr = R \sin(\theta - \gamma) d\varpi / \cos^2 \varpi$. Thus,

$$\begin{aligned}
& \int_0^\infty \frac{1}{\{R^2 + r^2 - 2rR \cos(\theta - \gamma)\}^{1/2}} r dr \\
&= \frac{1}{9R^9} + \frac{\cos(\theta - \gamma)}{R^9 \sin^{10}(\theta - \gamma)} \left[\frac{128}{315} + \cos(\theta - \gamma) \left\{ \frac{1}{9} \sin^8(\theta - \gamma) + \frac{8}{63} \sin^6(\theta - \gamma) \right\} \right. \\
&\quad \left. + \frac{16}{105} \sin^4(\theta - \gamma) + \frac{64}{315} \sin^2(\theta - \gamma) + \frac{128}{315} \right].
\end{aligned} \tag{A.6}$$

Integrating with respect to θ is carried out as

$$\begin{aligned}
& \int_\pi^{2\pi} \frac{1}{9R^9} + \frac{\cos(\theta - \gamma)}{R^9 \sin^{10}(\theta - \gamma)} \left[\frac{128}{315} + \cos(\theta - \gamma) \left\{ \frac{1}{9} \sin^8(\theta - \gamma) + \frac{8}{63} \sin^6(\theta - \gamma) \right\} \right. \\
&\quad \left. + \frac{16}{105} \sin^4(\theta - \gamma) + \frac{64}{315} \sin^2(\theta - \gamma) + \frac{128}{315} \right] d\theta \\
&= \frac{1}{R^9} \left[-\frac{128}{2835} \frac{1}{\sin^9 \omega} - \frac{1}{9} \cot \omega - \cot^3 \omega \left\{ \frac{8}{81} + \frac{16}{189} \csc^2 \omega + \frac{64}{945} \csc^4 \omega + \frac{128}{2835} \csc^6 \omega \right\} \right]_{\pi - \gamma}^{2\pi - \gamma} \\
&= \frac{256}{2835} \frac{1}{R^9 \sin^9 \gamma}.
\end{aligned} \tag{A.7}$$

The final result is

$$\therefore \int_\pi^{2\pi} \int_0^\infty \int_{-\infty}^\infty \frac{1}{MN^{12}} r dz dr d\theta = \frac{\pi}{45} \frac{1}{R^9 \sin^9 \gamma}. \tag{A.8}$$

This together with the attractive potential component from Wu and Wong (2004) gives

$$\begin{aligned}
\Phi_{fs} &= \iiint_{V_s} n_s \phi_{fs} dV = \int_{\pi}^{2\pi} \int_0^{\infty} \int_{-\infty}^{\infty} \left(\frac{n_s \nu_{fs}}{MN^{12}} - \frac{n_s \beta_{fs}}{MN^6} \right) r dz dr d\theta \\
&= \frac{\pi}{45} \frac{n_s \nu_{fs}}{R^9 \sin^9 \gamma} - \frac{\pi}{6} \frac{n_s \beta_{fs}}{R^3 \sin^3 \gamma} \\
&= \frac{\pi}{45} \frac{n_s \nu_{fs}}{v_1^9} - \frac{\pi}{6} \frac{n_s \beta_{fs}}{v_1^3},
\end{aligned} \tag{A.9}$$

where $v_1 (= R \sin \gamma)$ is the height of the molecular M from the solid substrate (Fig. 2.2).

The interactive potential between the liquid molecule and the gas region is

$$\Phi_{fg} = \iiint_{V_s} n_g \phi_{fg} dV = \int_{\psi}^{\pi} \int_0^{\infty} \int_{-\infty}^{\infty} \frac{n_g \nu_{fg}}{MN^{12}} - \frac{n_g \beta_{fg}}{MN^6} r dz dr d\theta \tag{A.10}$$

The only difference is the boundary conditions in angle θ . Using Eq. (A.6) with the new conditions

$$\begin{aligned}
\Phi_{fg} &= \int_{\psi}^{\pi} \frac{1}{9R^9} + \frac{\cos(\theta - \gamma)}{R^9 \sin^{10}(\theta - \gamma)} \left[\frac{128}{315} + \cos(\theta - \gamma) \left\{ \frac{1}{9} \sin^8(\theta - \gamma) + \frac{8}{63} \sin^6(\theta - \gamma) \right\} \right. \\
&\quad \left. + \frac{16}{105} \sin^4(\theta - \gamma) + \frac{64}{315} \sin^2(\theta - \gamma) + \frac{128}{315} \right] d\theta \\
&= \frac{1}{R^9} \left[-\frac{128}{2835} \frac{1}{\sin^9 \omega} - \frac{1}{9} \cot \omega - \cot^3 \omega \left\{ \frac{8}{81} + \frac{16}{189} \csc^2 \omega + \frac{64}{945} \csc^4 \omega + \frac{128}{2835} \csc^6 \omega \right\} \right]_{\psi - \gamma}^{\pi - \gamma} \\
&= \frac{1}{2835 R^9 \sin^9 \omega} \left[-128 - 315 \cos \omega \sin^8 \omega - \cos^3 \omega \sin^6 \omega \right. \\
&\quad \left. + \{ 280 + 240 \csc^2 \omega + 192 \csc^4 \omega + 128 \csc^6 \omega \} \right]_{\psi - \gamma}^{\pi - \gamma} \\
&= \frac{1}{2835 R^9 \sin^9 \omega} \left[128 + 315 \cos \omega - 420 \cos^3 \omega + \right. \\
&\quad \left. + \{ 378 \cos^5 \omega - 180 \cos^7 \omega + 35 \cos^9 \omega \} \right]_{\psi - \gamma}^{\pi - \gamma} \tag{A.11}
\end{aligned}$$

Thus,

$$\Phi_{fg} = \frac{\pi n_g \nu_{fg}}{11520} \left(\frac{b_1 - 256}{v_1^9} + \frac{b_2}{v_2^9} \right) - \frac{\pi n_g \beta_{fg}}{6} \left(\frac{a_1 - 1}{v_1^3} + \frac{a_2}{v_2^3} \right). \tag{A.12}$$

$$\begin{aligned}
a_1 &= \frac{1}{2} + \frac{3}{4} \cos \gamma - \frac{1}{4} \cos^3 \gamma \\
a_2 &= \frac{1}{2} + \frac{3}{4} \cos(\psi - \gamma) - \frac{1}{4} \cos^3(\psi - \gamma) \\
b_1 &= 128 + 315 \cos \gamma - 420 \cos^3 \gamma + 378 \cos^5 \gamma - 180 \cos^7 \gamma + 35 \cos^9 \gamma \\
b_2 &= 128 + 315 \cos(\psi - \gamma) - 420 \cos^3(\psi - \gamma) + 378 \cos^5(\psi - \gamma) \\
&\quad - 180 \cos^7(\psi - \gamma) + 35 \cos^9(\psi - \gamma)
\end{aligned} \tag{A.13}$$

where $v_2 (= R \sin(\psi - \gamma))$ is the distance from M to the liquid-vapor interface (Fig. 2.2).

Φ_{ff} is easily found by using the two previous results in Eq. (A.9) and (A.12). Let Φ_{-D} be the intermolecular potential between M and an infinite body of liquid V_{-D} outside a sphere of radius D surrounding M , and this potential is expressed by

$$\Phi_{-D} = \iiint_{V_{-D}} n_f \phi_{ff} dV = \int_D^\infty \left(\frac{n_f \nu_{ff}}{r^{12}} - \frac{n_f \beta_{ff}}{r^6} \right) (4\pi r^2) r dr = \frac{4\pi n_f \nu_{ff}}{9D^9} - \frac{4\pi n_f \beta_{ff}}{3D^3}.$$

(A.14)

Let Φ_c be the intermolecular potential between M and a liquid occupying the vapor and solid regions and this potential is

$$\Phi_c = \frac{\pi n_f \nu_{ff}}{45 v_1^9} + \frac{\pi n_f \nu_{ff}}{11520} \left(\frac{b_1 - 256}{v_1^9} + \frac{b_2}{v_2^9} \right) - \frac{\pi n_f \beta_{ff}}{6 v_1^3} - \frac{\pi n_f \beta_{ff}}{6} \left(\frac{a_1 - 1}{v_1^3} + \frac{a_2}{v_2^3} \right). \tag{A.15}$$

After summing these two terms, I get the interactive potential between the liquid molecule and the liquid region as follows:

$$\begin{aligned}
\Phi_{ff} &= \Phi_{-D} - \Phi_c \\
&= \frac{4\pi n_f \nu_{ff}}{9D^9} - \frac{\pi n_f \nu_{ff}}{11520} \left(\frac{b_1}{v_1^9} + \frac{b_2}{v_2^9} \right) - \frac{4\pi n_f \beta_{ff}}{3D^3} + \frac{\pi n_f \beta_{ff}}{6} \left(\frac{a_1}{v_1^3} + \frac{a_2}{v_2^3} \right).
\end{aligned} \tag{A.16}$$

Because this potential is relative, I neglect the constant terms in Eq. (A.16).

The total intermolecular potential per unit volume at the liquid molecular M in the liquid is

found by summing Eq. (A.9), (A.13), and (A.16):

$$\begin{aligned}\Phi_{total} &= n_f (\Phi_{fs} + \Phi_{fg} + \Phi_{ff}) \\ &= -\frac{\pi n_f^2 \nu_{ff}}{11520} \left(\frac{b_1(1-\zeta) + 256(\zeta - \varphi)}{v_1^9} + \frac{b_2(1-\zeta)}{v_2^9} \right) \\ &\quad + \frac{\pi n_f^2 \beta_{ff}}{6} \left(\frac{a_1(1-\rho) + \rho - \lambda}{v_1^3} + \frac{a_2(1-\rho)}{v_2^3} \right)\end{aligned}\tag{A.17}$$

$$\varphi = \frac{n_s \nu_{fs}}{n_f \nu_{ff}}, \zeta = \frac{n_g \nu_{fg}}{n_f \nu_{ff}}, \lambda = \frac{n_s \beta_{fs}}{n_f \beta_{ff}}, \rho = \frac{n_g \beta_{fg}}{n_f \beta_{ff}}.\tag{A.18}$$

APPENDIX B

EXCESS ENERGY AND INTERACTION POTENTIAL

The total intermolecular potential in Appendix A includes both thin-film and bulk contributions. However, we are only interested in the thin-film part. The bulk component is calculated by taking the particle M in Fig. 2.2 far away from the solid substrate. To find the bulk component Φ_∞ , we assume $v_1 = y \rightarrow \infty$ in the total intermolecular potential Φ_{total} . In this limit, the four parameters in Eq. (A.12) become $a_1 \rightarrow \frac{1}{2}$, $a_2 \rightarrow 1$, $b_1 \rightarrow 128$, $b_2 \rightarrow 256$. The bulk component is derived by substituting these values into Eq. (A.17).

$$\begin{aligned}\Phi_\infty &= \frac{256\pi n_f n_g v_{fg}}{11520v_2^9} - \frac{256\pi n_f^2 v_{ff}}{11520v_2^9} - \frac{\pi n_f n_g \beta_{fg}}{6v_2^3} + \frac{\pi n_f^2 \beta_{ff}}{6v_2^3} \\ &= -\frac{\pi n_f^2 v_{ff}}{45v_2^9}(1-\zeta) + \frac{\pi n_f^2 \beta_{ff}}{6v_2^3}(1-\rho).\end{aligned}\tag{B.1}$$

Thus, the net interactive potential is

$$\begin{aligned}\Phi_{total} - \Phi_\infty &= -\frac{\pi n_f^2 v_{ff}}{11520} \left(\frac{b_1(1-\zeta) + 256(\zeta - \varphi)}{v_1^9} + \frac{(b_2 - 256)(1-\zeta)}{v_2^9} \right) \\ &\quad + \frac{\pi n_f^2 \beta_{ff}}{6} \left(\frac{a_1(1-\rho) + \rho - \lambda}{v_1^3} + \frac{(a_2 - 1)(1-\rho)}{v_2^3} \right).\end{aligned}\tag{B.2}$$

The excess energy is found by integration of this net potential from h to D . This integration is done separately for the repulsive and attractive components.

$$\begin{aligned}
E &= \int_D^h (\Phi - \Phi_\infty) dy \\
&= \int_D^h \left[-\frac{\pi n_f^2 \nu_{ff}}{11520} \left(\frac{b_1(1-\zeta) + 256(\zeta - \varphi)}{v_1^9} + \frac{(b_2 - 256)(1-\zeta)}{v_2^9} \right) \right. \\
&\quad \left. + \frac{\pi n_f^2 \beta_{ff}}{6} \left(\frac{a_1(1-\rho) + \rho - \lambda}{v_1^3} + \frac{(a_2 - 1)(1-\rho)}{v_2^3} \right) \right] dy.
\end{aligned} \tag{B.3}$$

From Fig. 2.2 we get

$$\begin{aligned}
\cos \gamma &= \frac{h}{(h^2 + h_x^2 y^2)^{1/2}} \quad \text{and} \quad \cos(\psi - \gamma) = \left[\frac{(h_x y + h)^2}{(1 + h_x^2)(h^2 + h_x^2 y^2)} \right]^{1/2}, \\
\sin \gamma &= \frac{h_x y}{(h^2 + h_x^2 y^2)^{1/2}} \quad \text{and} \quad \sin(\psi - \gamma) = \left[\frac{h_x^2 (h - y)^2}{(1 + h_x^2)(h^2 + h_x^2 y^2)} \right]^{1/2}.
\end{aligned} \tag{B.4}$$

The repulsive excess energy is calculated by integration of the potential in Eq. (B.3):

$$E_{rep} = \int_D^h \frac{\pi n_f^2 \nu_{ff}}{11520} \left[\frac{(b_1 - 256)(\zeta - 1)}{v_1^9} + \frac{256(\varphi - 1)}{v_1^9} + \frac{(b_2 - 256)(\zeta - 1)}{v_2^9} \right] dy. \tag{B.5}$$

Each term inside the bracket in Eq. (B.5) is calculated separately.

$$\begin{aligned}
(\zeta - 1) \int_D^h \frac{b_1 - 256}{v_1^9} dy &= \\
(\zeta - 1) \left(\frac{\left\{ \begin{array}{l} -35h_x^6 - 70h_x^4 - 56h_x^2 - 16 \\ + 16(1 + h_x^2)^{1/2} (h_x^2 + 1)^3 \end{array} \right\}}{(1 + h_x^2)^{7/2} h^8} - Z_1 \right),
\end{aligned} \tag{B.6}$$

$$256(\varphi - 1) \int_D^h \frac{1}{v_2^9} dy = 32(1 - \varphi) \left(\frac{1}{h^8} - \frac{1}{D^8} \right) \tag{B.7}$$

$$\begin{aligned}
(\zeta - 1) \int_D^h \frac{b_2 - 256}{v_2^9} dy &= \\
\left(-\frac{128h_x^{16} + 448h_x^{14} + 560h_x^{12} + 280h_x^{10} + 35h_x^8}{8(1 + h_x^2)^{7/2} h^8} - Z_2 \right) (\zeta - 1).
\end{aligned} \tag{B.8}$$

where Z_1 and Z_2 are functions of D, h , and h_x . Exact expressions of these two terms are given in Appendix G.2. In this paper, we assume $D/h \ll 1$. The leading order terms of the repulsive component in the limit $D/h \rightarrow 0$ are

$$E_{rep} = \frac{\pi m_f^2 \nu_{ff}}{11520} \left(\begin{array}{l} \left(\zeta - 1 \right) \left(\frac{\left(-35h_x^6 - 70h_x^4 - 56h_x^2 - 16 + \right. \right.}{16(1+h_x^2)^{1/2}(h_x^6 + 3h_x^4 + 3h_x^2 + 1)} - \frac{35h_x^8}{8h^8} \right) - \\ \frac{32(\varphi-1)}{h^8} - \frac{32(\varphi-1)}{D^8} - \\ \left(\zeta - 1 \right) \left(\frac{128h_x^{16} + 448h_x^{14} + 560h_x^{12} + 280h_x^{10} + 35h_x^8}{8(1+h_x^2)^{7/2}h^8} \right) - \\ \left(\zeta - 1 \right) \left(\frac{35h_x^8 + 105h_x^6 + 126h_x^4 +}{72h_x^2 + 16 - 16(1+h_x^2)^{9/2}} \right) \end{array} \right). \quad (\text{B.9})$$

The term containing D is constant and can be dropped because E is a potential. In addition, this equation is expanded in the limit $h_x \rightarrow 0$ because of $h_x \ll 1$. Thus,

$$E = -\frac{\pi m_f^2 \nu_{ff} \{64(\varphi-1) + 63h_x^{10}(\zeta-1)\}}{23040h^8} + \frac{\pi m_f^2 \beta_{ff} \{8(\lambda-1) + 3h_x^{10}(\rho-1)\}}{96h^2}, \quad (\text{B.10})$$

where the attractive component from Wu and Wong(2004) has been included.

Excess energy expression is given by (B.10). Using new coefficients, I get this form as following

$$E = \frac{8T}{9h^8} \left(\frac{9}{8} \eta^{10} + \frac{1}{64} h_x^{10} \right) - \frac{4S}{3h^2} \left(\frac{3}{8} \alpha^4 + \frac{1}{8} h_x^4 \right). \quad (\text{B.11})$$

where

$$T = \frac{63\pi_f^2 \nu_{ff} (1-\varphi)}{320}, S = \frac{3\pi_f^2 \beta_{ff} (1-\rho)}{16}, \eta = \left(\frac{64(1-\varphi)}{567(1-\zeta)} \right)^{\frac{1}{10}}, \alpha = \left(\frac{8(1-\lambda)}{9(1-\rho)} \right)^{\frac{1}{4}}. \quad (\text{B.12})$$

APPENDIX C

ANALYTICAL SOLUTION OF UNIFORM FILMS

The augmented Young-Laplace equation with the slope and curvature set to zero becomes

$$C = -\varepsilon \left(\frac{1}{H^3} \right) + R \left(\frac{\xi^{10}}{H^9} \right) \quad \rightarrow \quad CH^9 + \varepsilon H^6 - R\xi^{10} = 0 \quad (\text{C.1})$$

There is no general method to find an analytical solution of the ninth order polynomial. However,

this problem can be converted into a cubic polynomial by defining a new parameter $W \equiv H^3$:

$$W^3 + \frac{\varepsilon}{C} W^2 - \frac{R\xi^{10}}{C} = 0. \quad (\text{C.2})$$

This cubic equation has an analytical solution.

$$\begin{aligned} W_1 &= (s_1 + s_2) - \frac{x_2}{3}, \\ W_2 &= -\frac{1}{2}(s_1 + s_2) - \frac{x_2}{3} + \frac{i\sqrt{3}}{2}(s_1 - s_2), \\ W_3 &= -\frac{1}{2}(s_1 + s_2) - \frac{x_2}{3} - \frac{i\sqrt{3}}{2}(s_1 - s_2). \end{aligned} \quad (\text{C.3})$$

$$s_1 = \left[r + (q^3 + r^2)^{\frac{1}{2}} \right]^{\frac{1}{3}}, \quad (\text{C.4})$$

$$s_2 = \left[r - (q^3 + r^2)^{\frac{1}{2}} \right]^{\frac{1}{3}}$$

$$r = -\frac{1}{2}x_0 - \frac{1}{27}x_2^3, \quad q = -\frac{1}{9}x_2^2, \quad (\text{C.5})$$

$$x_0 \equiv -\frac{R\xi^{10}}{C}, \quad x_2 \equiv \frac{\varepsilon}{C}.$$

Thus, $H = W^{1/3}$.

Out of the nine solutions of H , only three are real. To see this point, we expand the solutions.

Transforming Eq. (C.4) in the complex plane, we find

$$s_1 = \left[r + (q^3 + r^2)^{\frac{1}{2}} \right]^{\frac{1}{3}} = \left| \frac{\varepsilon}{3C} \right| \exp\left(\frac{(2n\pi + \theta)}{3} \right),$$

$$s_2 = \left[r - (q^3 + r^2)^{\frac{1}{2}} \right]^{\frac{1}{3}} = \left| \frac{\varepsilon}{3C} \right| \exp\left(\frac{(2n\pi + \theta')}{3} \right),$$

where

$$\theta = \tan^{-1} \frac{(-q^3 - r^2)^{\frac{1}{2}}}{r},$$

$$\theta' = \tan^{-1} \left(-\frac{(-q^3 - r^2)^{\frac{1}{2}}}{r} \right).$$

Thus,

$$H = \left\{ 2 \left| \frac{\varepsilon}{3C} \right| \cos\left(\frac{\theta}{3} \right) - \frac{\varepsilon}{3C} \right\}^{1/3},$$

$$\text{and } H = \left\{ 2 \left| \frac{\varepsilon}{3C} \right| \cos\left(\frac{\theta}{3} \pm \frac{2}{3}\pi \right) - \frac{\varepsilon}{3C} \right\}^{1/3}. \quad (\text{C.6})$$

When the expressions of q and r are substituted, we obtain

$$\frac{(-q^3 - r^2)^{\frac{1}{2}}}{r} = \frac{3\sqrt{3}C\sqrt{-R\xi^{10}(27R\xi^{10}C^2 - 4\varepsilon^3)}}{(27R\xi^{10}C^2 - 2\varepsilon^3)} \quad (\text{C.7})$$

By Taylor's expansion of θ ,

$$\theta = \tan^{-1} \left(\frac{(-q^3 - r^2)^{\frac{1}{2}}}{r} \right) = \frac{(-q^3 - r^2)^{\frac{1}{2}}}{r} - \frac{1}{3} \left(\frac{(-q^3 - r^2)^{\frac{1}{2}}}{r} \right)^3 + \frac{1}{5} \left(\frac{(-q^3 - r^2)^{\frac{1}{2}}}{r} \right)^5 + O \left(\left(\frac{(-q^3 - r^2)^{\frac{1}{2}}}{r} \right)^6 \right). \quad (\text{C.8})$$

Ignoring higher order terms and substituting Eq. (C.7) into θ , we find

$$\left\{ 2 \left| \frac{\varepsilon}{3C} \right| \cos \left(\frac{\theta}{3} \right) - \frac{\varepsilon}{3C} \right\}^{1/3} = - \left(\frac{\varepsilon}{C} \right)^{\frac{1}{3}} + \frac{\left(\frac{\varepsilon}{C} \right)^{\frac{1}{3}} C^2}{3\varepsilon^3} R_{\xi}^{\varepsilon^{10}} + \frac{7 \left(\frac{\varepsilon}{C} \right)^{\frac{1}{3}} C^4}{9\varepsilon^6} \left(R_{\xi}^{\varepsilon^{10}} \right)^2,$$

$$\left\{ 2 \left| \frac{\varepsilon}{3C} \right| \cos \left(\frac{\theta}{3} \pm \frac{2\pi}{3} \right) - \frac{\varepsilon}{3C} \right\}^{1/3} = \mp \left(\frac{1}{\varepsilon} \right)^{\frac{1}{6}} \left(R_{\xi}^{\varepsilon^{10}} \right)^{\frac{1}{6}} - \frac{C}{6\varepsilon^{\frac{5}{3}}} \left(R_{\xi}^{\varepsilon^{10}} \right)^{\frac{2}{3}} \mp \frac{13C^2}{72\varepsilon^{\frac{19}{6}}} \left(R_{\xi}^{\varepsilon^{10}} \right)^{\frac{7}{6}}.$$

In conclusion, we find real solutions of H :

$$H = \left\{ \begin{array}{l} - \left(\frac{\varepsilon}{C} \right)^{\frac{1}{3}} + \frac{\left(\frac{\varepsilon}{C} \right)^{\frac{1}{3}} C^2}{3\varepsilon^3} R_{\xi}^{\varepsilon^{10}} + \frac{7 \left(\frac{\varepsilon}{C} \right)^{\frac{1}{3}} C^4}{9\varepsilon^6} \left(R_{\xi}^{\varepsilon^{10}} \right)^2, \\ \left(\frac{1}{\varepsilon} \right)^{\frac{1}{6}} \left(R_{\xi}^{\varepsilon^{10}} \right)^{\frac{1}{6}} - \frac{C}{6\varepsilon^{\frac{5}{3}}} \left(R_{\xi}^{\varepsilon^{10}} \right)^{\frac{2}{3}} + \frac{13C^2}{72\varepsilon^{\frac{19}{6}}} \left(R_{\xi}^{\varepsilon^{10}} \right)^{\frac{7}{6}}, \\ - \left(\frac{1}{\varepsilon} \right)^{\frac{1}{6}} \left(R_{\xi}^{\varepsilon^{10}} \right)^{\frac{1}{6}} - \frac{C}{6\varepsilon^{\frac{5}{3}}} \left(R_{\xi}^{\varepsilon^{10}} \right)^{\frac{2}{3}} - \frac{13C^2}{72\varepsilon^{\frac{19}{6}}} \left(R_{\xi}^{\varepsilon^{10}} \right)^{\frac{7}{6}} \end{array} \right\}. \quad (\text{C.9})$$

The first one is the uniform film with unit height, the second is the precursor film, and the third is negative and is not physical.

APPENDIX D PERTURBATION SOLUTIONS OF PRECURSOR FILM

The thickness of uniform film is governed by Eq. (C.1):

$$CH^9 + \varepsilon H^6 - R\xi^{10} = 0 \quad (\text{D.1})$$

Here, we solve for H in the limit $R\xi^{10} \rightarrow 0$. If $R\xi^{10} = 0$, then Eq. (D.1) becomes

$$H_0^6 \left(H_0^3 + \frac{\varepsilon}{C} \right) = 0 \quad (\text{D.2})$$

The real solutions are $H_0 = 0$ and $H_0 = (-\varepsilon/C)^{1/3}$ (the dimensionless pressure difference $C < 0$ and the parameter $\varepsilon > 0$). Thus, we have to expand the governing equation Eq. (D.1) differently for their two branches.

If $H_0 = (-\varepsilon/C)^{1/3}$, we rescale the governing equation (D.1) by defining $h = H/H_0$:

$$h^9 - h^6 + \delta_1 = 0, \quad (\text{D.3})$$

where $\delta_1 = (C^2 R \xi^{10} / \varepsilon^3) \ll 1$.

To find an asymptotic solution of Eq. (D.3), we expand h as

$$h = h_0 + \delta_1 h_1 + \delta_1^2 h_2 + \dots \quad (\text{D.4})$$

Substituting this h into Eq. (D.3), and equating the δ_1 yields

$$\begin{aligned} 0 &= h_0^9 - h_0^6, \\ 0 &= (9h_0^8 - 6h_0^5)h_1 + 1, \\ 0 &= (36h_0^8 - 15h_0^4)h_1^2 + (9h_0^8 - 6h_0^5)h_2. \end{aligned} \quad (\text{D.5})$$

Thus,

$$\begin{aligned}
h_0 &= 1, \\
h_1 &= -\frac{1}{3}, \\
h_2 &= -\frac{7}{9}.
\end{aligned} \tag{D.6}$$

and

$$h = 1 - \frac{1}{3} \left(\frac{C^2 R \xi^{10}}{\varepsilon^3} \right) - \frac{7}{9} \left(\frac{C^2 R \xi^{10}}{\varepsilon^3} \right)^2. \tag{D.7}$$

This gives

$$H = \left(-\frac{\varepsilon}{C} \right)^{\frac{1}{3}} \left\{ 1 - \frac{1}{3} \left(\frac{C^2 R \xi^{10}}{\varepsilon^3} \right) - \frac{7}{9} \left(\frac{C^2 R \xi^{10}}{\varepsilon^3} \right)^2 \right\} \tag{D.8}$$

This is the uniform film with unit height. It agrees with the first solution in Eq. (C.9).

The other branch $H_0=0$ leads to the precursor film. By balancing the attractive and repulsive components of disjoining pressure in Eq. (D.1), we get $H = (R \xi^{10} / \varepsilon)^{1/6} \ll 1$. If we define

$\delta_2 = R \xi^{10} / \varepsilon$, and $h = H / \delta_2^{1/6}$, then the governing equation becomes

$$(C \delta_2^{1/2} / \varepsilon) h^9 + h^6 - 1 = 0. \tag{D.9}$$

We expand h as

$$h = h_0 + \delta_2^{1/2} h_1 + \delta_2 h_2. \tag{D.10}$$

Substituting into Eq. (D.9) and equating coefficients yields

$$\begin{aligned}
h_0^6 - 1 &= 0, \\
(C / \varepsilon) h_0^9 + 6 h_0^5 h_1 &= 0, \\
0 &= \left(9(C / \varepsilon) h_0^8 h_1 + 15 h_0^4 h_1^2 + 6 h_0^5 h_2 \right)
\end{aligned} \tag{D.11}$$

Thus,

$$h = 1 - \delta_2^{\frac{1}{2}} \left(\frac{Ch_0^4}{6\varepsilon} \right) + \delta_2 \left(\frac{13h_0^7 C^2}{72\varepsilon^2} \right). \quad (\text{D.12})$$

This gives

$$H = \left(\frac{R\xi^{10}}{\varepsilon} \right)^{\frac{1}{6}} - \frac{C}{6\varepsilon} \left(\frac{R\xi^{10}}{\varepsilon} \right)^{\frac{2}{3}} + \frac{13C}{72\varepsilon} \left(\frac{R\xi^{10}}{\varepsilon} \right)^{\frac{7}{6}} + \dots \quad (\text{D.14})$$

This agrees with the solution of the precursor film in Eq. (C.9).

APPENDIX E
ASYMPTOTIC SOLUTIONS OF PRECURSOR FILM THICKNESS AND C_2

The precursor film thickness H obeys Eq. (D.14).

$$-\frac{(1+H)}{2H^2} + \left(\frac{R\xi^{10}}{\varepsilon}\right) \frac{(1+H)(1+H^2)(1+H^4)}{8H^8} + \frac{1}{H^3} - \left(\frac{R\xi^{10}}{\varepsilon}\right) \frac{1}{H^9} = 0, \quad (\text{E.1})$$

Let $(R\xi^{10}/\varepsilon)^{1/6} \equiv \delta \ll 1$. Thus, $H = H(\delta)$ and we can expand H as

$$H = H_0 + H_1\delta + H_2\delta^2 + H_3\delta^3 + H_4\delta^4 + H_5\delta^5 + H_6\delta^6 + O(\delta^7). \quad (\text{E.2})$$

When this series is substituted into Eq. (E.1), we find

$$H_0 = 0, H_1 = 1, H_2 = \frac{1}{24}, H_3 = \frac{29}{288}, H_4 = \frac{3415}{82944}, H_5 = \frac{36353}{1327104}, H_6 = \frac{4014713}{191102976}. \quad (\text{E.3})$$

The pressure difference C_2 that yields a precursor film is related to the film thickness by

$$C = -\frac{\varepsilon}{H^3} + \frac{R\xi^{10}}{H^9}.$$

Substituting H into this equation, then

$$C \approx -\frac{\varepsilon}{\delta^3} \left(1 - \frac{1}{8}\delta\right) + \frac{R\xi^{10}}{\delta^9} \left(1 - \frac{3}{8}\delta\right) \approx -\frac{\varepsilon}{4\delta^2} + \dots \quad (\text{E.4})$$

APPENDIX F
RELATIONS BETWEEN TWO CRITICAL CAPILLARY PRESSURE
DIFFERENCES (C_1, C_2)

The pressure difference C_1 yields a uniform film of unit height and C_2 generates a drop with an unbounded precursor film. These two critical values are given by

$$C_1 = -\varepsilon + R\xi^{10}, \quad (\text{F.1})$$

$$C_2 = -\frac{\varepsilon}{H^3} + \frac{R\xi^{10}}{H^9}. \quad (\text{F.2})$$

Before comparing C_1 and C_2 , we have to find the ratio $R\xi^{10}/\varepsilon$. Since R, ξ and ε all depend on the intermolecular potential, we use another form of the Lennard-Jones potential:

$$\phi(r) = 4e \left[\left(\frac{r_0}{r} \right)^{12} - \left(\frac{r_0}{r} \right)^6 \right], \quad (\text{F.3})$$

where e is the well depth and r_0 is the collision diameter. This form is compared to that in Eq.

(A.1) and the strengths of the repulsive and attractive components become

$$\begin{aligned} \nu &= 4er_0^{12}, \\ \beta &= 4er_0^6. \end{aligned} \quad (\text{F.4})$$

The parameters R, ξ and ε are defined in Eq. (3.6), and the ratio

$$\frac{R\xi^{10}}{\varepsilon} = \frac{2(n_f e_{ff} r_{0,ff}^{12} - n_s e_{sf} r_{0,fs}^{12})}{15(n_f e_{ff} r_{0,ff}^6 - n_s e_{sf} r_{0,fs}^6)(h_0)^6} = \frac{2}{15} \left(\frac{r_0}{h_0} \right)^6 \ll 1, \quad (\text{F.5})$$

where we have assumed $r_{0,ff} = r_{0,fs} = r_0$. Since h_0 is the maximum height of the drop and

$h_0 \gg r_0$, the ratio $R\xi^{10}/\varepsilon \ll 1$.

To compare C_1 and C_2 , we define $f = C_1 - C_2$ and substitute Eq. (F.1) and (F.2) in f :

$$f = -\varepsilon + R\xi^{10} - \left\{ -\frac{\varepsilon}{H^3} + \frac{R\xi^{10}}{H^9} \right\}$$

$$= \frac{\varepsilon(1-H^3)}{H^3} [H^6 - \delta(H^6 + H^3 + 1)]. \quad (\text{F.6})$$

If $H = 1, f = 0$ and $C_1 = C_2$. If $H < 1$, then for $f > 0$, we need

$$H^6 - \delta(H^6 + H^3 + 1) > 0. \quad (\text{F.7})$$

This is transformed into

$$(H^3 - H_1^3)(H^3 - H_2^3) > 0, \quad (\text{F.8})$$

where

$$H_1^3 = \frac{\delta - \sqrt{\delta^2 + 4\delta(1-\delta)}}{2(1-\delta)}, \quad (\text{F.9})$$

$$H_2^3 = \frac{\delta + \sqrt{\delta^2 + 4\delta(1-\delta)}}{2(1-\delta)}. \quad (\text{F.10})$$

Thus, we need either (1) $H > H_1$ and $H > H_2$ or (2) $H < H_1$ and $H < H_2$. Since $H_1 < 0$, the second condition is unphysical. Thus, for $f > 0$, we need $1 > H > H_2$. The condition $H_2 < 1$ gives

$$3\delta^2 - 4\delta + 1 > 0$$

$$\text{or } (3\delta - 1)(\delta - 1) > 0. \quad (\text{F.11})$$

Since $\delta < 1$, this requires $\delta < 1/3$. Thus, for $C_1 > C_2$, we only need $\delta < 1/3$, which is satisfied in general as shown by Eq. (F.5).

APPENDIX G COMPUTER PROGRAMS

G.1. The Fourth-order Runge-Kutta Code

```
//Main Numerical methods (4th order Runge-Kutta method)

//To find the shape of 2nd order differential equation. (From "the augmented Young-Laplace
equation")

#include <stdio.h>

#include <math.h>

const long double          c=-0.01+0.001*0.00000543,delta=+0.00001;

const long double ep=0.01,ka=0.001,mu=0.00000543,d=0.01,xmax=3.2,h1=1.0;

const long double bb=(13.0*ep*pow(h1,5.0)+15.0*c/pow(h1,2.0))/(6.0*ep/pow(h1,4.0)+9.0*c
/h1);

long double Equation1(long double x, long double h, long double hx)

{

return(c*pow(h,9.0)+ep*(1.0-pow(hx,4.0))*pow(h,6.0)-a*mu+ka*pow(hx,10.0))/(1*pow(h,9.0)-
2.0*pow(h,7.0)*ep*hx*hx+5.0/4.0*h*ka*pow(hx,8.0));

}
```

```
long double Equation1(long double,long double,long double);           //Using L-J potential
```

```
void main()
```

```
{
```

```
    FILE * fp ;
```

```
    fp=fopen("D:/workdata/data.txt","wt");
```

```
{
```

```
    long double j=0;
```

```
    for (j=0.0;j<1.0;j=j+1.0)
```

```
    {
```

```
        //printf("\n step size=");
```

```
        //scanf("%Lf",&d);
```

```
        //printf("\n max. x=");
```

```
        //scanf("%Lf",&xmax);
```

```
        long double x0=0.0, b=0.1 ,hxi0=delta*22.12565357+pow(delta,2)*(b*22.12565357-  
2*22.12565357*20.60948424);
```

```
        long double h0=h1+delta+delta*delta*(b-bb);
```

```
        long double hi=h0, hxi=hxi0, hi1=h0, hxi1=hxi0;
```

```
        long double xi,k1,k2,k3,k4,l1,l2,l3,l4,kk1,kk2,kk3,kk4,ll1,ll2,ll3,ll4;
```

```

for(xi=x0;xi<xmax;xi=xi+d)

{

fprintf(fp,"\n %.3lf %.16lf ",(xi),hi1);

printf("\n %.3lf %.16lf ",(xi),hi1);

        kk1=hxi1;

        ll1=Equation1(xi,hi1,hxi1);

        kk2=hxi1+d*ll1/2.0;

        ll2=Equation1(xi+d/2.0,hi1+kk1*d/2.0,hxi1+ll1*d/2.0);

        kk3=hxi1+d*ll2/2.0;

        ll3=Equation1(xi+d/2.0,hi1+kk2*d/2.0,hxi1+ll2*d/2.0);

        kk4=hxi1+d*ll3;

        ll4=Equation1(xi+d,hi1+kk3*d,hxi1+ll3*d);

        hxi1=hxi1+d*(ll1+2.0*ll2+2.0*ll3+ll4)/6.0;

        hi1=hi1+d*(kk1+2.0*kk2+2.0*kk3+kk4)/6.0;    //Using L-J potential

        if (hi1>20.0)

                hi1=0.0;

```

```
        if (hi1<0.0)
            hi1=0.0;
    }

    printf("\n\n");
}

fclose(fp);
}
}
```

G.2. Maple Code for Appendix A and B

> restart:

> a1:=h/(h^2+hx^2*y^2)^(1/2):

> a2:=(hx*y+h)/(1+hx^2)^(1/2)/(h^2+hx^2*y^2)^(1/2):

> b1:=hx*y/(h^2+hx^2*y^2)^(1/2):

> b2:=hx*(h-y)/(1+hx^2)^(1/2)/(h^2+hx^2*y^2)^(1/2):

> c1:=128+315*a1-420*a1^3+378*a1^5-180*a1^7+35*a1^9:

> c2:=128+315*a2-420*a2^3+378*a2^5-180*a2^7+35*a2^9:

> d1:=int((c1-256)/y^9,y):

> d2:=subs(y=h-t,d1):

> Z1:=subs(y=D,d1):

$$Z1 := - \frac{1}{(hx^2 D^2 + h^2) D^8} \left(35 hx^6 D^6 h^2 - 16 \sqrt{hx^2 D^2 + h^2} hx^6 D^6 \right. \\ \left. + 70 hx^4 D^4 h^3 - 48 \sqrt{hx^2 D^2 + h^2} hx^4 D^4 h^2 + 56 hx^2 D^2 h^5 \right. \\ \left. - 48 \sqrt{hx^2 D^2 + h^2} hx^2 D^2 h^4 + 16 h^7 - 16 \sqrt{hx^2 D^2 + h^2} h^6 \right)$$

> d4:=subs(t=1/s,d2):

> d5:=subs(D=h/s,Z1):

> assume(h>0):

> e1:=simplify(limit(asympt(d4,s,11),s=infinity)):

> e2:=limit(simplify(asympt(d5,s,11)),s=infinity):

>x01:=(e1-e2)*(q-1):x02:=(-35*hx^6-70*hx^4-56*hx^2-

16)/((1+hx^2)^(7/2)*h^8)+(16*hx^6+48*hx^4+48*hx^2+16)/((1+hx^2)^3*h^8)-35/8*hx^8/h^8:

> x1:=x02*(q-1);

$$x1 := \left(\frac{-35 hx^6 - 70 hx^4 - 56 hx^2 - 16}{(1 + hx^2)^{7/2} h^8} + \frac{16 hx^6 + 48 hx^4 + 48 hx^2 + 16}{(1 + hx^2)^3 h^8} - \frac{35 hx^8}{8 h^8} \right) (q - 1)$$

> d6:=int(1/y^9,y):

> d7:=subs(y=h-t,d6):d8:=subs(y=D,d6):

> d9:=subs(t=1/s,d7):

> d10:=subs(D=h/s,d8):

> e3:=simplify(limit(asympt(d9,s,11),s=infinity)):

> x2:=256*((e3-d8))*(p-1);

$$x2 := 256 \left(-\frac{1}{8 h^8} + \frac{1}{8 D^8} \right) (p - 1)$$

> f1:=h+hx^2*y:f2:=1+hx^2:f3:=h^2+hx^2*y^2:f4:=h-y:

> v2:=f6*f3^(-1/2):

- > g1:=-128*f2^(9/2)/f4^9:
- > g2:=315*f1*f2^4/f3^(1/2)/f4^9:
- > g3:=-420*f1^3*f2^3/f3^(3/2)/f4^9:
- > g4:=378*f1^5*f2^2/f3^(5/2)/f4^9:
- > g5:=-180*f1^7*f2/f3^(7/2)/f4^9:
- > g6:=35*f1^9/f3^(9/2)/f4^9:
- > i1:=int(g1,y):j01:=subs(y=h-t,i1):j1:=subs(y=D,i1):
- > i2:=int(g2,y):j02:=subs(y=h-t,i2):j2:=subs(y=D,i2):
- > i3:=int(g3,y):j03:=subs(y=h-t,i3):j3:=subs(y=D,i3):
- > i4:=int(g4,y):j04:=subs(y=h-t,i4):j4:=subs(y=D,i4):
- > i5:=int(g5,y):j05:=subs(y=h-t,i5):j5:=subs(y=D,i5):
- > i6:=int(g6,y):j06:=subs(y=h-t,i6):j6:=subs(y=D,i6):
- > k1:=j01+j02+j03+j04+j05+j06:Z2:=j1+j2+j3+j4+j5+j6;

$$Z2 := - \frac{1}{h^8 (-h+D)^8 (h^2 + hx^2 D^2)^{(7/2)} \sqrt{1+hx^2}} \left(-72 h^{15} \sqrt{1+hx^2} hx^2 \right. \\
+ 16 hx^{16} D^{15} \sqrt{1+hx^2} + 80 h^{14} \sqrt{h^2 + hx^2 D^2} hx^2 \\
+ 160 h^{14} \sqrt{h^2 + hx^2 D^2} hx^4 + 160 h^{14} \sqrt{h^2 + hx^2 D^2} hx^6 \\
\left. + 80 h^{14} \sqrt{h^2 + hx^2 D^2} hx^8 + 16 h^{14} \sqrt{h^2 + hx^2 D^2} hx^{10} \right)$$

$$\begin{aligned}
& -126 h \sim^{15} h x^4 \sqrt{1+h x^2} - 105 h \sim^{15} h x^6 \sqrt{1+h x^2} \\
& -35 h \sim^{15} h x^8 \sqrt{1+h x^2} + 448 h x^{16} h \sim^2 \sqrt{1+h x^2} D^{13} \\
& +56 h x^{14} h \sim^2 \sqrt{1+h x^2} D^{13} - 560 h x^{12} h \sim^5 \sqrt{1+h x^2} D^{10} \\
& -448 h x^{14} h \sim^3 \sqrt{1+h x^2} D^{12} + 875 h x^{10} h \sim^8 \sqrt{1+h x^2} D^7 \\
& -35 h x^8 h \sim^8 \sqrt{1+h x^2} D^7 + 2009 h \sim^{10} h x^{10} \sqrt{1+h x^2} D^5 \\
& +48 h \sim^{12} \sqrt{h \sim^2 + h x^2 D^2} h x^2 D^2 + 48 h \sim^{10} \sqrt{h \sim^2 + h x^2 D^2} h x^4 D^4 \\
& +16 h \sim^8 \sqrt{h \sim^2 + h x^2 D^2} h x^6 D^6 - 3136 h x^{14} h \sim^5 \sqrt{1+h x^2} D^{10} \\
& -896 h x^{16} h \sim^3 \sqrt{1+h x^2} D^{12} + 1568 h x^{14} h \sim^4 \sqrt{1+h x^2} D^{11} \\
& +240 h \sim^{12} \sqrt{h \sim^2 + h x^2 D^2} h x^4 D^2 + 240 h \sim^{10} \sqrt{h \sim^2 + h x^2 D^2} h x^6 D^4 \\
& +80 h \sim^8 \sqrt{h \sim^2 + h x^2 D^2} h x^8 D^6 + 480 h \sim^{12} \sqrt{h \sim^2 + h x^2 D^2} h x^6 D^2 \\
& +480 h \sim^{10} \sqrt{h \sim^2 + h x^2 D^2} h x^8 D^4 + 160 h \sim^8 \sqrt{h \sim^2 + h x^2 D^2} h x^{10} D^6 \\
& +480 h \sim^{12} \sqrt{h \sim^2 + h x^2 D^2} h x^8 D^2 + 480 h \sim^{10} \sqrt{h \sim^2 + h x^2 D^2} h x^{10} D^4 \\
& +160 h \sim^8 \sqrt{h \sim^2 + h x^2 D^2} h x^{12} D^6 + 240 h \sim^{12} \sqrt{h \sim^2 + h x^2 D^2} h x^{10} D^2 \\
& +240 h \sim^{10} \sqrt{h \sim^2 + h x^2 D^2} h x^{12} D^4 + 80 h \sim^8 \sqrt{h \sim^2 + h x^2 D^2} h x^{14} D^6 \\
& +48 h \sim^{12} \sqrt{h \sim^2 + h x^2 D^2} h x^{12} D^2 + 48 h \sim^{10} \sqrt{h \sim^2 + h x^2 D^2} h x^{14} D^4 \\
& +16 h \sim^8 \sqrt{h \sim^2 + h x^2 D^2} h x^{16} D^6 + 448 h x^{16} D^9 h \sim^6 \sqrt{1+h x^2} \\
& +1708 h x^{12} h \sim^{10} \sqrt{1+h x^2} D^5 - 896 h x^{16} \sqrt{1+h x^2} h \sim^5 D^{10} \\
& -35 h \sim^{14} h x^8 \sqrt{1+h x^2} D + 1960 h x^{12} D^9 h \sim^6 \sqrt{1+h x^2}
\end{aligned}$$

$$\begin{aligned}
& - 56 h \sim^{13} h x^2 \sqrt{1+h x^2} D^2 - 245 h \sim^{10} h x^8 \sqrt{1+h x^2} D^5 \\
& + 35 h x^{10} D^9 h \sim^6 \sqrt{1+h x^2} - 280 h x^{10} h \sim^7 \sqrt{1+h x^2} D^8 \\
& + 3920 h x^{14} D^9 h \sim^6 \sqrt{1+h x^2} - 252 h \sim^{13} h x^4 \sqrt{1+h x^2} D^2 \\
& - 441 h \sim^{13} h x^6 \sqrt{1+h x^2} D^2 - 35 h \sim^9 h x^8 \sqrt{1+h x^2} D^6 \\
& - 1960 h \sim^9 h x^{10} \sqrt{1+h x^2} D^6 - 3920 h \sim^9 h x^{12} \sqrt{1+h x^2} D^6 \\
& - 448 h \sim^9 h x^{14} \sqrt{1+h x^2} D^6 - 315 h \sim^{11} h x^6 \sqrt{1+h x^2} D^4 \\
& - 35 h \sim^9 h x^6 \sqrt{1+h x^2} D^6 - 70 h \sim^{11} h x^4 \sqrt{1+h x^2} D^4 \\
& + 1496 h x^{14} h \sim^8 \sqrt{1+h x^2} D^7 + 1120 h x^{16} h \sim^4 \sqrt{1+h x^2} D^{11} \\
& - 560 h \sim^{11} h x^{12} \sqrt{1+h x^2} D^4 - 128 h x^{16} \sqrt{1+h x^2} h \sim D^{14} \\
& + 70 h x^{12} D^{11} h \sim^4 \sqrt{1+h x^2} - 280 h \sim^{13} h x^{10} \sqrt{1+h x^2} D^2 \\
& + 16 h \sim^{14} \sqrt{h \sim^2 + h x^2} D^2 - 16 h \sim^{15} \sqrt{1+h x^2} \\
& + 665 h \sim^{12} h x^{10} \sqrt{1+h x^2} D^3 + 4774 h x^{12} h \sim^8 \sqrt{1+h x^2} D^7 \\
& - 1960 h \sim^{11} h x^{10} \sqrt{1+h x^2} D^4 - 245 h \sim^{11} h x^8 \sqrt{1+h x^2} D^4 \\
& - 3136 h x^{14} h \sim^7 \sqrt{1+h x^2} D^8 - 128 h x^{16} h \sim^7 \sqrt{1+h x^2} D^8 \\
& - 245 h \sim^{13} h x^8 \sqrt{1+h x^2} D^2 - 245 h \sim^{12} h x^8 \sqrt{1+h x^2} D^3 \\
& - 3920 h x^{12} h \sim^7 \sqrt{1+h x^2} D^8)
\end{aligned}$$

> l1:=subs(t=1/s,k1):l2:=subs(D=h/s,Z2):

> assume(h>0):

> m1:=asympt(l1,s,9):

> m2:=simplify(m1):

> n1:=convert(m2,polynomial):

> n2:=limit(asympt(l2,s,9),e=infinity):

> x3:=(n1-n2)*(q-1);

$$x3 := \left(-\frac{128 hx^{16} + 448 hx^{14} + 560 hx^{12} + 280 hx^{10} + 35 hx^8}{8 (1 + hx^2)^{(7/2)} h^8} - \frac{35 hx^8 + 105 hx^6 + 126 hx^4 + 72 hx^2 + 16 - 16 (1 + hx^2)^{(9/2)}}{h^8} \right) (q - 1)$$

>E01:=(pi*n[f]^2*alpha[ff]/11520)*(x1+simplify(x2-256*(p-1)/8/D^8)+x3);

$$E01 := \frac{1}{11520} \pi n_f^2 \alpha_{ff} \left(\left(\frac{-35 hx^6 - 70 hx^4 - 56 hx^2 - 16}{(1 + hx^2)^{(7/2)} h^8} + \frac{16 hx^6 + 48 hx^4 + 48 hx^2 + 16}{(1 + hx^2)^3 h^8} - \frac{35 hx^8}{8 h^8} \right) (q - 1) - \frac{32 (p - 1)}{h^8} \right. \\ \left. + \left(-\frac{128 hx^{16} + 448 hx^{14} + 560 hx^{12} + 280 hx^{10} + 35 hx^8}{8 (1 + hx^2)^{(7/2)} h^8} - \frac{35 hx^8 + 105 hx^6 + 126 hx^4 + 72 hx^2 + 16 - 16 (1 + hx^2)^{(9/2)}}{h^8} \right) (q - 1) \right)$$

> E001:=subs(hx=1/tt,E01);

$$E001 := \frac{1}{11520} \pi n_f^2 \alpha_{ff} \left(\left(\frac{-\frac{35}{t^6} - \frac{70}{t^4} - \frac{56}{t^2} - 16}{\left(1 + \frac{1}{t^2}\right) h^8} + \frac{\frac{16}{t^6} + \frac{48}{t^4} + \frac{48}{t^2} + 16}{\left(1 + \frac{1}{t^2}\right)^3 h^8} - \frac{35}{8 h^8 t^8} \right) (q-1) - \frac{32(p-1)}{h^8} \right. \\ \left. + \left(\frac{\frac{128}{t^{16}} + \frac{448}{t^{14}} + \frac{560}{t^{12}} + \frac{280}{t^{10}} + \frac{35}{t^8} \frac{35}{t^8} + \frac{105}{t^6} + \frac{126}{t^4} + \frac{72}{t^2} + 16 - 16 \left(1 + \frac{1}{t^2}\right)^{(9/2)}}{8 \left(1 + \frac{1}{t^2}\right) h^8} - \frac{}{h^8} \right) (q-1) \right)$$

> E002:=asympt(E001,tt,12):E003:=subs(tt=1/hx,E002):E1:=convert(E003,polynomial);

$$E1 := -\frac{\pi n_f^2 \alpha_{ff} (p-1)}{360 h^8} - \frac{7 \pi n_f^2 \alpha_{ff} (q-1) h x^{10}}{2560 h^8}$$

>E2:=-pi*n[f]^2*beta[ff]*(1-rho)/32/h^2*((1-lambda)*8/(1-rho)/3+hx^4);

$$E2 := -\frac{\pi n_f^2 \beta_{ff} (1-\rho) \left(\frac{8(1-\lambda)}{3(1-\rho)} + h x^4 \right)}{32 h^2}$$

> E:=simplify(E1)+E2;

$$E := -\frac{\pi n_f^2 \alpha_{ff} (64p - 64 + 63 h x^{10} q - 63 h x^{10})}{23040 h^8} - \frac{\pi n_f^2 \beta_{ff} (1-\rho) \left(\frac{8(1-\lambda)}{3(1-\rho)} + h x^4 \right)}{32 h^2}$$

> PI1:=diff(E,h):

> PI2:=subs(hx=u(x),diff(E,hx)):PI3:=subs(h=h(x),PI2):

> PI4:=diff(PI3,x):PI6:=(subs(u(x)=hx,PI4)):

> PI7:=subs(diff(h(x),x)=hx,subs(diff(u(x),x)=hxx,-PI1+PI4)):

> PI:=sort(PI7,h);

$$\Pi := - \frac{\pi n_f^2 \beta_{\mathcal{G}}(1-\rho) \left(\frac{8(1-\lambda)}{3(1-\rho)} + hx^4 \right)}{16 h^3} - \frac{\pi n_f^2 \alpha_{\mathcal{G}}(5670 u(x)^8 q hxx - 5670 u(x)^8 hxx)}{23040 h^8} + \frac{\pi n_f^2 \beta_{\mathcal{G}}(1-\rho) u(x)^3 hx}{4 h(x)^3}$$

$$- \frac{3 \pi n_f^2 \beta_{\mathcal{G}}(1-\rho) u(x)^2 hxx}{8 h(x)^2}$$

G.3. Boundary Conditions at the Contact Point

Start with this equation:

$$\lim_{h \rightarrow 0} \left(E - h_x \frac{\partial E}{\partial h_x} \right) = \lim_{h \rightarrow 0} \left[\frac{T}{8} \left(\frac{\eta^{10} - h_x^{10}}{h^8} \right) - \frac{S}{2} \left(\frac{\alpha^4 - h_x^4}{h^2} \right) \right] = \lim_{h \rightarrow 0} \left[\frac{\text{Numerator}}{\text{Denominator}} \right].$$

Using Maple to apply the l'Hospital's rule, we find the boundary conditions at $h \rightarrow 0$:

> <Numerator>

> f:=(T*(eta^10-diff(h(x),x)^10)-4*S*h(x)^6*(alpha^4-diff(h(x),x)^4)):

> subs(diff(h(x),x\$1)=hx,h(x)=0,f);

$$T \left(\eta^{10} - h_x^{10} \right)$$

$$\rightarrow |h_x| \rightarrow \eta$$

> f1:=simplify(diff(f,x)):

> subs(diff(h(x),x\$2)=hxx,diff(h(x),x\$1)=eta,h(x)=0,f1);

$$-10 \eta^9 T h_{xx}$$

$$\rightarrow h_{xx} \rightarrow 0$$

> f2:=collect(diff(f1,x),diff(h(x),x\$3)):

> subs(diff(h(x),x\$3)=hxxx,diff(h(x),x\$2)=0,diff(h(x),x)=eta,h(x)=0,f2);

$$-10 \eta^9 T h_{xxx}$$

$$\rightarrow h_{xxx} \rightarrow 0$$

> f3:=collect(diff(f2,x),diff(h(x),x\$4)):

> subs(diff(h(x),x\$4)=hxxxx,diff(h(x),x\$3)=0,diff(h(x),x\$2)=0,diff(h(x),x)=eta,h(x)=0,f3);

$$-10 \eta^9 T h_{xxxx}$$

$$\rightarrow h_{xxxx} \rightarrow 0$$

> f4:=collect(diff(f3,x),diff(h(x),x\$5)):

>

subs(diff(h(x),x\$5)=hxxxxx,diff(h(x),x\$4)=0,diff(h(x),x\$3)=0,diff(h(x),x\$2)=0,diff(h(x),x)=eta,h(x)=0,f4);

$$-10 \eta^9 T h_{xxxxx}$$

$$\rightarrow h_{xxxxx} \rightarrow 0$$

> f5:=collect(diff(f4,x),diff(h(x),x\$6)):

>

subs(diff(h(x),x\$6)=hxxxxxx,diff(h(x),x\$5)=0,diff(h(x),x\$4)=0,diff(h(x),x\$3)=0,diff(h(x),x\$2)=0,diff(h(x),x)=eta,h(x)=0,f5);

$$-10 \eta^9 T h_{xxxxxx}$$

$$\rightarrow h_{xxxxxx} \rightarrow 0$$

> f6:=collect(diff(f5,x),diff(h(x),x\$7)):

>

subs(diff(h(x),x\$7)=hxxxxxxx,diff(h(x),x\$6)=0,diff(h(x),x\$5)=0,diff(h(x),x\$4)=0,diff(h(x),x\$3)=0,diff(h(x),x\$2)=0,diff(h(x),x)=eta,h(x)=0,f6);

$$-10 \eta^9 T h_{xxxxxxx} - 2 \eta \left(-1440 S \eta^9 + 1440 S \eta^5 \alpha^4 \right)$$

$$\rightarrow h_{xxxxxxx} \rightarrow \frac{288S(\eta^4 - \alpha^4)}{T\eta^3}$$

> f7:=collect(diff(f6,x),diff(h(x),x\$8)):

> subs(diff(h(x),x\$8)=hxxxxxxxx,diff(h(x),x\$7)=eta*(-

1440*S*eta^9+1440*S*eta^5*alpha^4)/(-

5)/eta^9/T,diff(h(x),x\$6)=0,diff(h(x),x\$5)=0,diff(h(x),x\$4)=0,diff(h(x),x\$3)=0,diff(h(x),x\$2)=0,

diff(h(x),x)=eta,h(x)=0,f7);

$$-10 \eta^9 T h_{xxxxxxxx}$$

$$\rightarrow h_{xxxxxxxx} \rightarrow 0$$

> f8:=collect(diff(f7,x),diff(h(x),x\$9)):

> subs(diff(h(x),x\$9)=hxxxxxxxxx,diff(h(x),x\$8)=0,diff(h(x),x\$7)=eta*(-

1440*S*eta^9+1440*S*eta^5*alpha^4)/(-

5)/eta^9/T,diff(h(x),x\$6)=0,diff(h(x),x\$5)=0,diff(h(x),x\$4)=0,diff(h(x),x\$3)=0,diff(h(x),x\$2)=0,

diff(h(x),x)=eta,h(x)=0,f8);

$$-10 \eta^9 T h_{xxxxxxxx}$$

$$\rightarrow h_{xxxxxxxx} \rightarrow 0$$

>

> **<Denominator>**

> den:=diff(h(x)^8,x\$8):

> subs(diff(h(x),x)=eta,h(x)=0,den);

$$40320 \eta^8$$

Finally, evaluation of limitation at the contact point becomes zero.

VITA

The author, Taeil Yi, was born in August 1977, in Seoul, Republic of Korea. He graduated from Hansung Science High School in February 1996.

In March 1996, the author attended Hanyang University with a major in mechanical engineering. He completed his army service in February 2000. He obtained a bachelor's degree in mechanical engineering in February 2003.

In August 2003, the author furthered his graduate study in the Department of Mechanical Engineering, Louisiana State University. And in December 2005, the degree of Master of Science in Mechanical Engineering will be conferred.